

# Bethe $M$ -layer construction for the percolation problem

Maria Chiara Angelini<sup>1,2</sup>, Saverio Palazzi<sup>1,\*</sup>, Tommaso Rizzo<sup>1,3</sup>, Marco Tarzia<sup>4,5</sup>

**1** Dipartimento di Fisica, Sapienza Università di Roma, Piazzale A. Moro 2, I-00185, Rome, Italy

**2** INFN-Sezione di Roma 1, Piazzale A. Moro 2, 00185, Rome, Italy

**3** ISC-CNR, UOS Rome, Sapienza Università di Roma, Piazzale A. Moro 2, I-00185, Rome, Italy

**4** LPTMC, CNRS-UMR 7600, Sorbonne Université, 4 Pl. Jussieu, F-75005 Paris, France

**5** Institut Universitaire de France, 1 rue Descartes, 75231 Paris Cedex 05, France

★ saverio.palazzi@uniroma1.it

## Abstract

The major difference between percolation and other phase transition models is the absence of an Hamiltonian and of a partition function. For this reason it is not straightforward to identify the corresponding field theory to be used as starting point of Renormalization Group computations. Indeed, it could be identified with the field theory of  $n+1$  states Potts model in the limit of  $n \rightarrow 0$  only by means of the mapping discovered by Kasteleyn and Fortuin for bond percolation. In this paper we show that it is possible to recover the epsilon expansion for critical exponents in finite dimension directly using the  $M$ -layer expansion, without the need to perform any analytical continuation. Moreover, we also show explicitly that the critical exponents for site and bond percolation are the same. This computation provides a reference for applications of the  $M$ -layer method to systems where the underlying field theory is unknown or disputed.

## 1 Introduction

The percolation problem provides one of the simplest example of a second-order phase transition, in both the versions of site or bond percolation. Despite the simplicity of the model, it is at the basis of different problems in many different fields, from condensed matter to telecommunication engineering, from graph theory to epidemic spreading [1, 2]. In the standard site (bond) percolation problem, each site (bond) is present independently of the neighbors with probability  $p$ . Above a certain threshold  $p_c$ , a giant cluster of nearest neighbor sites is present in the thermodynamic limit while below this threshold neighboring sites are grouped in many small clusters of non-extensive size.  $p_c$  corresponds to the transition point, and one can associate standard critical exponents that describe how critical observables behave near  $p_c$ . In spite of the deep similarities with respect to critical behavior, the main difference between percolation and other phase transition models is the absence of an associated Hamiltonian and a corresponding partition function.

The renormalization group (RG) is the main tool to study second order phase transition. It can be applied in two ways: the first one is by performing explicitly a RG transformation on a given two- or three-dimensional lattice while the second relies on field theory. The first method typically requires uncontrolled approximations (needed to close

the RG equations and find a fixed point) while the second is more powerful as it allows to obtain systematically the critical exponents in dimension  $D$  in powers of  $\epsilon = D_c - D$  where  $D_c$  is the upper critical dimension. The first method can be applied to percolation as it is [3, 4] but one could think that the lack of a Hamiltonian would make the application of the second impossible. However in a seminal paper Kasteleyn and Fortuin showed that the bond-percolation problem is exactly related to the  $n \rightarrow 0$  limit of an  $n$ -component ( $n + 1$  states) Potts model [5]. It was then recognized [6] that this mapping allows the application of field-theoretical techniques and today the exponents are known up to the 5th order in an  $\epsilon$ -expansion around the upper critical dimension [7–11].

In this paper, we reproduce the same expansion up to one-loop order by means of the  $M$ -layer construction. The  $M$ -layer construction has been introduced in ref. [12], and then applied to a variety of models [13–18]. The useful property of the  $M$ -layer construction is that one can study the critical behavior, in finite dimensions, of problems which are not defined by a Hamiltonian, such as the percolation. One has to introduce  $M - 1$  additional independent lattices, in addition to the original one; the  $M$  layers will then be coupled together through a random rewiring of the bonds. The  $M \rightarrow \infty$  limit gives the Bethe lattice solution [19] of the model, while if  $M = 1$  one obtains the original model. An expansion in  $1/M$  can be properly set up, that is in practice an expansion in the number of the topological loops considered. The  $M$ -layer construction can be applied to any model that can be defined on the Bethe lattice, including percolation. This is interesting, because, with this approach, there is no need to invoke the  $n \rightarrow 0$  analytic continuation discovered by Kasteleyn and Fortuin. Furthermore, with this method, we can also analytically verify that the critical exponents of site percolation are equal to those of bond percolation.

The additional value of this paper is methodological: we show for the first time that from the  $1/M$  expansion on the  $M$ -layer lattice one can obtain the epsilon expansion, through the suitable introduction of an adimensional beta function in analogy with what is usually done in standard field theory [20, 21]. This is a fundamental step that will help in applying in the future the same techniques to more complicated systems, for which a finite-dimensional solution is still not known, such as the Edward-Anderson spin-glass model [17] or Anderson localization [18].

The paper is organized as follows: In section 2 we present the model and the main results, in particular we sketch the derivation of the epsilon expansion for the critical exponents from the  $1/M$  expansion of two- and three-point correlation functions. In section 3 we introduce the problem on the Bethe lattice with a novel derivation of the cluster distribution function. In section 4 we recall the general properties of the  $1/M$  expansion and the operative rules to compute it. In section 5 we present the actual computation for site percolation. In section 6 we briefly show how the same computation easily generalize to the case of bond percolation. In section 7 we give our conclusions.

## 2 Models and Main results

In this section, we list the results of the application of the  $M$ -layer construction to both the bond and site percolation problems on an hyper-cubic lattice in  $D$  dimensions. We briefly describe the steps needed to reach the final results which will be summarized next.

In the standard site (respectively bond) percolation problem, each site (respectively bond) is present (or active) independently of the neighbors with probability  $p$ . In the site percolation problem one then defines a cluster as a subset of nearest-neighbour active sites, while in bond percolation a cluster is defined as a subset of sites connected by nearest-neighbour active bonds. At  $p_c$  a giant cluster appears, that contains a finite fraction of

all the sites  $N$ . Our analysis will mainly apply to the non-percolating phase  $p < p_c$  and from now on we refer to this case. The critical behavior in the non-percolating phase is characterized by considering the average number  $n(s, p)$  of clusters of size  $s$  in a system of size  $N$ . This distribution is cut off at a typical size  $s^*$  that diverges at the critical point. We also consider the function  $C_k(x_1, \dots, x_k)$  that gives the probability that the points  $x_1, \dots, x_k$  belong to the same cluster. According to scaling arguments [1, 22], we expect that the two-point function obeys the following scaling form for large  $|x_1 - x_2|$  and for  $p$  close to  $p_c$ :

$$C_2(x_1, x_2) = \frac{1}{|x_1 - x_2|^{D-2+\eta}} f_{C_2} \left( \frac{|x_1 - x_2|}{\xi} \right) \quad (1)$$

where  $f_{C_2}$  is a proper scaling function,  $\eta$  is the anomalous dimension and  $\xi$  is the correlation length that diverges at the critical point as:

$$\xi \propto \frac{1}{|p - p_c|^\nu}. \quad (2)$$

The typical size  $s^*$  scales with the correlation length as

$$s^* \propto \xi^{D_f}, \quad (3)$$

where  $D_f$  stands for fractal dimension of the clusters. The distribution of the cluster sizes also obeys a scaling law [1, 22]:

$$n(s, p) = s^{-\tau} f_n((p - p_c)s^\sigma), \quad (4)$$

where  $f_n(x)$  is another scaling-function and the critical exponents  $\tau$  and  $\sigma$  are related to  $\nu$  and  $D_f$  through:

$$\tau = D/D_f + 1, \quad \sigma = \frac{1}{\nu D_f}. \quad (5)$$

We consider the space integrals of the  $C_k(x_1, \dots, x_k)$ , also called susceptibilities,

$$\chi_k \equiv \sum_{x_2, \dots, x_k} C_k(x_1, \dots, x_k) \quad (6)$$

that are independent of  $x_1$  in a homogeneous system. They are related to the moments of the  $n(s, p)$  through:

$$\chi_k = \sum_{s=0}^{\infty} s^k n(s, p). \quad (7)$$

One can easily see that the scaling law obeyed by  $n(s, p)$  implies that the susceptibilities diverge as:

$$\chi_k \propto \xi^{-D+D_f k}, \quad (8)$$

from which it follows that the following quantity goes to a constant at the critical point:

$$\lambda \propto \xi^{-D} \frac{\chi_3^2}{\chi_2^3}. \quad (9)$$

On the  $M$ -layer lattice  $\chi_2$  and  $\chi_3$  are given by the Bethe lattice result in the limit  $M \rightarrow \infty$  and we computed the first  $1/M$  correction, for both site and bond percolation, this allows to write  $\lambda$  as:

$$\lambda = u - \frac{7}{4} \frac{u^2}{(4\pi)^{\frac{D}{2}}} \Gamma \left( 3 - \frac{D}{2} \right). \quad (10)$$

The constant  $u$  is defined as  $u \equiv g m^{D-6}$ , where  $m \equiv \xi^{-1}$  and  $g$  is a  $\mathcal{O}(1/M)$  constant that depends on the microscopic details of the model including whether we consider bond or site percolation. Note that the adimensional constant  $u$  diverges at the critical point for  $D < 6$  because  $m$  vanishes, while  $\lambda$  remains finite at the critical point according to Eq. (8). More precisely we expect that:

$$\lambda \approx \lambda_c + c_1 \xi^\omega = \lambda_c + c_1 m^{-\omega}, \quad \xi \rightarrow \infty, m \rightarrow 0 \quad (11)$$

where  $c_1$  is a model dependent constant while  $\omega$  is a universal exponent that controls the corrections to scaling [20]. Now following a standard field-theoretical procedure (see ref. [20], chap. 8) we define the function  $b(\lambda)$ . The above relationships imply:

$$b(\lambda) \equiv m^2 \frac{\partial}{\partial m^2} \lambda \approx -\frac{\omega}{2} c_1 m^{-\omega} \approx -\frac{\omega}{2} (\lambda - \lambda_c), \quad (12)$$

meaning that at the critical point

$$b(\lambda_c) = 0, \quad \omega = -2b'(\lambda_c) \quad (13)$$

From (10), we obtain an expression of  $b(\lambda)$  to second order in  $\lambda$  from which the following scenario emerges: for  $D \geq D_u = 6$  only the solution  $\lambda = 0$  exists meaning that  $\lambda$  tends to zero at the critical point with  $\omega = 6 - D$ , while for  $\epsilon \equiv 6 - D > 0$  a new solution  $\lambda_c \neq 0$  appears:

$$\lambda_c = \frac{2(4\pi)^3}{7} \epsilon + \mathcal{O}(\epsilon^2) \quad (14)$$

and  $\lambda$  tends to  $\lambda_c$  at the critical point with  $\omega = -\epsilon + \mathcal{O}(\epsilon^2)$ . Following similar standard computations (see ref. [20], Chap. 8), from the value of  $\lambda_c$  and the scaling laws, we obtained the  $\epsilon$ -expansion for the critical exponents:

$$\nu = \frac{1}{2} + \frac{5}{84} \epsilon + \mathcal{O}(\epsilon^2), \quad (15)$$

$$\eta = -\frac{1}{21} \epsilon + \mathcal{O}(\epsilon^2). \quad (16)$$

Comparing Eq. (8) with the scaling law  $\chi_2 \propto \xi^{2-\eta}$  we obtain

$$D_f = \frac{D + 2 - \eta}{2}, \quad (17)$$

all the other critical exponents can be obtained from  $\eta$  and  $\nu$  through the scaling laws given above. Note that the result is independent of the actual value of the constant  $g$  ensuring that the critical exponents are model independent and in particular they are the same for bond and site percolation. As it should, the results coincide with those obtained from the  $\epsilon$ -expansion for the  $(n+1)$ -state Potts models in the limit  $n \rightarrow 0$ , which coincides with bond percolation according to the Fortuin-Kasteleyn mapping. In appendix D we have also computed the expansion of  $\chi_4$  in powers of  $1/M$  checking that it diverges at the critical point with an exponent equal to that predicted by Eq. (8).

### 3 Percolation on the Bethe Lattice

In this section we will show how to write exact equations for the critical behavior of important observables for site percolation on a Bethe lattice, and how to derive the exact

critical exponents in this case. Here and in the following we call as Bethe lattice a random regular graph with fixed connectivity  $c$ .

Given  $g(s, p) = s n(s, p)/p$  that is the probability that a randomly chosen site belongs to a cluster of size  $s$ , we define the cavity probability  $g_{cav}(s, p)$  accordingly on a site where one of its edges is removed. The cavity probability obeys the following self-consistent equation on the Bethe lattice with fixed connectivity  $c$ :

$$g_{cav}(s, p) = (1 - p) \delta_{s,0} + p \sum_{s_1=0}^{\infty} \cdots \sum_{s_{c-1}=0}^{\infty} g_{cav}(s_1, p) \cdots g_{cav}(s_{c-1}, p) \delta_{s, 1+s_1+\cdots+s_{c-1}}. \quad (18)$$

The probability  $g(s, t)$  can then be expressed in terms of the cavity probability as:

$$g(s, p) = (1 - p) \delta_{s,0} + p \sum_{s_1=0}^{\infty} \cdots \sum_{s_c=0}^{\infty} g_{cav}(s_1, p) \cdots g_{cav}(s_c, p) \delta_{s, 1+s_1+\cdots+s_c}. \quad (19)$$

Next we define the generating function  $\tilde{g}(t, p) \equiv \sum_{s=0}^{\infty} g(s, p) e^{-ts}$  and its cavity counterpart. Eq. (18) becomes:

$$\tilde{g}_{cav}(t, p) = (1 - p) + p (\tilde{g}_{cav}(t, p))^{c-1} e^{-t}. \quad (20)$$

Deriving the above equation with respect to  $t$  and setting  $t = 0$  we obtain

$$\tilde{g}'_{cav}(0, p) = \frac{p}{p(c-1) - 1} \quad (21)$$

from which we obtain

$$\chi_2(p) = -p g'(0, p) = \frac{p^2(p+1)}{1 - p(c-1)} \quad (22)$$

that diverges, as expected, at the critical point  $p_c = 1/(c-1)$ . We are interested in the functions  $g(s, p)$  for  $p$  close to the critical point and  $s$  large that corresponds to small values of  $t$  in  $\tilde{g}(t, p)$ . We now define

$$\delta \tilde{g}(t, p) \equiv \tilde{g}(t, p) - 1 \quad (23)$$

and its cavity counterpart  $\delta \tilde{g}_{cav}(t, p) \equiv \tilde{g}_{cav}(t, p) - 1$ . Differentiating Eq. (20) with respect to  $t$  we obtain, for small values of  $t$  and  $p$  close to  $p_c$ :

$$\delta \tilde{g}'_{cav}(t, p) (1 - p/p_c - (c-2) \delta \tilde{g}_{cav}(t, p)) = -p_c, \quad (24)$$

from which we obtain

$$\delta \tilde{g}_{cav}(t, p) = a (1 - (1 + t/t^*)^{1/2}) \quad (25)$$

where

$$\delta p \equiv p - p_c \quad a \equiv -\delta p \frac{c-1}{c-2}, \quad t^* \equiv \delta p^2 \frac{(c-1)^3}{2c-4}. \quad (26)$$

We also obtain (for small values of  $t$  and  $\delta p$ )

$$\delta \tilde{g}(t, p) = \frac{c}{c-1} \delta \tilde{g}_{cav}(t, p). \quad (27)$$

Now we have:

$$\delta \tilde{g}(t, p) = \sum_{s=0}^{\infty} g(s, p) (e^{-st} - 1) \quad (28)$$

replacing the sum with an integral (which is justified by the fact that small values of  $t$  correspond to large values of  $s$ ) we obtain, computing the inverse Laplace transform of (25),

$$g(s, p) \sim \frac{1}{s^{3/2}} e^{-st^*} \rightarrow n(s, p) \sim \frac{1}{s^{5/2}} e^{-st^*}, \quad (29)$$

that obeys Eq. (4) with exponents

$$\sigma = \frac{1}{2}, \quad \tau = \frac{5}{2} \quad (30)$$

that we identify with the mean-field values. In the next section we will consider percolation on the  $M$ -layer random lattice in finite dimension  $D$ . In the limit  $M \rightarrow \infty$  the function  $n(s, p)$  of the  $M$ -layer becomes identical to that of the Bethe lattice and therefore  $\tau = 5/2$  and  $\sigma = 1/2$ . In addition, we will show that for  $M \rightarrow \infty$  the two-point function obeys the scaling form (1) with exponents

$$\nu = \frac{1}{2}, \quad \eta = 0, \quad (31)$$

in all dimensions  $D \geq 2$ . Note that these relationships are consistent with (5) only for  $D = D_u = 6$ . Indeed  $\tau = D/D_f + 1$  is an hyperscaling relationship that is not generically valid [22] at variance with the more general  $\sigma^{-1} = \nu D_f$ , which implies  $D_f = 4$  for the  $M \rightarrow \infty$  model in any dimension. Computing the  $1/M$  corrections around the  $M \rightarrow \infty$  limit, we will show that for  $M$  *finite* the critical exponents are the same of the  $M \rightarrow \infty$  limit for  $D \geq D_u = 6$  while they are different for  $D < D_u = 6$ . On the other hand for  $D < 6$  both relationships (5) hold. We note that the  $M \rightarrow \infty$  model plays essentially the role of the Gaussian model in ferromagnetism, see [20] chapters four and five.

## 4 The $M$ -layer expansion

Conceptually the  $M$ -layer method is rather straightforward: 1) one introduce a  $D$  dimensional random lattice depending on a parameter  $M$ , the limit  $M \rightarrow \infty$  of the model is solvable as it coincides with the Bethe lattice solution; 2) then one computes the finite- $M$  corrections in powers of  $1/M$  around the Bethe lattice solution. The goal is to study the critical behaviour near a second order phase transition for a model on a given lattice and, as we anticipated in section (2), from the  $1/M$  expansion one can obtain the epsilon expansion. The  $M$ -layer expansion has been introduced in ref. [12] where diagrammatic rules were derived to compute the  $1/M$  corrections, in this section we recall these rules, referring to the original paper for their derivation and all the details. Note that percolation itself is particularly useful to understand the origin of these rules and it is treated as an example in section D of [12].

One can build the so-called  $M$ -layer construction considering  $M$  different layers of the original model, and then rewiring the bonds between each nearest neighboring node among the layers in such a way that each node on each layer still has the same number of neighbors, that now can be placed at different layers. In the following we will focus on hyper-cubic lattices with connectivity  $2D$ , even if the  $M$ -layer construction can be applied to any type of lattice. At the end of the procedure, the number of topological loops in the  $M$ -layer lattice will typically be reduced and in the  $M \rightarrow \infty$  limit there will be no loops of finite length: the  $M \rightarrow \infty$  solution of the model will correspond to the Bethe solution [19], computed on a random regular tree-like graph with the same fixed connectivity of the original model. At this point we can expand around this Bethe solution, introducing the

small parameter  $1/M$ . The original model corresponds to  $M = 1$ , thus in principle one should need all orders in  $1/M$  to obtain the correct solution for the original model. However, we are interested in the critical behaviour of the model, that should be independent on the actual value of  $M$  due to universality. This expectation will indeed be confirmed in the context of percolation by the present computation. Furthermore this implies that at each order in the  $1/M$  expansion we only need to consider the contributions that diverge the most approaching the critical point. One can show that the  $1/M$  expansion for a generic observable corresponds to an expansion in the number of topological loops considered when computing that observable. In particular, if one wants to compute the  $1/M$  expansion for a generic observable  $O$ , the following steps are required:

- *Step 1: Identify the possible topological diagrams*

Depending on the order at which one wants to perform the expansion, one should identify the possible topological diagrams over which one needs to compute the chosen observable. If one is interested in the leading order, one should only look at diagrams without loops, that corresponds to the Bethe locally tree-like topology. If one wants to compute the next-to-leading order, one has to identify all the possible topological diagrams that correspond to a Bethe lattice in which it has been manually injected a single topological loop, while any additional topological loop inserted will bring a new factor  $1/M$  in the expansion.

- *Step 2: Weights, number of projections and symmetry factors*

For any diagram  $\mathcal{G}$  identified in Step 1, one needs to associate to it:

- a weight  $W(\mathcal{G})$ , that will be a power of  $1/M$  and will indicate the probability that a topological diagram of that kind is obtained in the rewiring procedure;
- a symmetry factor  $S(\mathcal{G})$ , completely equivalent to that introduced in field theory for Feynman diagrams [21], that takes into account the number of ways in which vertices and lines can be switched leaving the topological structure of the diagram unaltered;
- the number of realizations of the chosen topological diagram on the original lattice,  $\mathcal{N}(\mathcal{G})$ : just as an example, if the chosen diagram is a line of length  $L$  between two points  $x_1$  and  $x_2$ , the number of such diagrams in the  $M$ -layered lattice having a different projection on the original lattice corresponds to the number of non-backtracking paths (NBP) of length  $L$  between the two points and its analytical expression is known in the literature [12, 23]. One can define  $\mathcal{N}_L(x_1, x_2, \hat{\mu}, \hat{\nu})$  as the number of NBP of length  $L$  where the directions  $\hat{\mu}$  and  $\hat{\nu}$  of the lines entering respectively in the external points  $x_1$  and  $x_2$  is fixed to one among the  $2D$  possible ones. In the large  $L$  limit, the actual value of the number of NBP will be independent on those directions, and we will simply define this number as  $\mathcal{N}_L(x_1, x_2)$ . The total number of the simple line diagrams of length  $L$  between two points  $x_1$  and  $x_2$  will thus be  $\mathcal{N}(\mathcal{G}) = (2D)^2 \mathcal{N}_L(x_1, x_2)$ , where the factor  $(2D)^2$  counts the possible entering directions of the line in the two external points. If one has a more complex diagram, to identify  $\mathcal{N}(\mathcal{G})$  it is sufficient to multiply a factor  $\mathcal{N}_L(x_i, x_j)$  for each internal line of length  $L$ , a factor  $2D$  for each external vertex and a factor  $\frac{(2D)!}{(2D-k)!}$  for any internal vertex of degree  $k$ , to count the different possible directions of the lines entering the vertex.

- *Step 3: Computation of the line-connected observable on the chosen diagram*

For any diagram  $\mathcal{G}$  identified in Step 1, one then needs to compute the value  $O(\mathcal{G})$  of the chosen observable computed on a Bethe lattice in which the topological structure of that diagram has been manually injected. This observable will depend on the topology of the diagram and on the length of the lines. One then need to compute the *line-connected* observable [12], subtracting to  $O(\mathcal{G})$  the value of the observable computed on the sub-graphs  $\mathcal{G}' \subset \mathcal{G}$  with proper coefficients in such a way that the final line-connected observable tends to zero if any line of  $\mathcal{G}$  has a diverging length.

- *Step 4: Sum of the contributions*

At the end, we need to sum the contributions to the chosen observable coming from the different chosen diagrams. Because the values of the chosen observable only depend on the projection of the considered diagrams, for each diagram  $\mathcal{G}$ , we multiply the value of the line-connected observable  $O_{lc}(\mathcal{G})$  by  $\mathcal{N}(\mathcal{G})$ ,  $S(\mathcal{G})$ ,  $W(\mathcal{G})$ , and we sum over the position of internal vertices and over the length of the internal lines.

## 5 *M-layer on site percolation in $D$ dimensions*

In this section, we apply the procedure described in the previous section to the percolation problem. We consider firstly the problem of site percolation on a hypercubic lattice in  $D$  dimensions, which we denote  $a_l \mathbb{Z}^D$ , considering  $a_l$  the lattice spacing. Following the notation of Sec. 2 we define  $p$  (where  $0 < p \leq 1$ ) as the probability that a site is present. Since the *M-layer* approach is a way to construct an expansion for observables around the Bethe solution, we define the “bare mass”

$$\mu \equiv -\ln \left( \frac{p}{p_c} \right) \quad \text{for } p \sim p_c, \quad (32)$$

where  $p_c = 1/(2D - 1)$  is the critical value for site percolation on a Bethe lattice with branching ratio  $2D - 1$ , above which the so-called “giant cluster” is present.

Following the prescriptions of the *M-layer* construction [12, 24] we report here the results of the application to the site percolation problem in the non-percolating phase,  $p < p_c$ . We are interested in two observables: the two and three-point correlation functions  $\overline{C_2(x_1, x_2)}$  and  $\overline{C_3(x_1, x_2, x_3)}$ , where  $\overline{\cdot}$  we denote the average over the rewirings of the *M-layer* procedure; According to the *M-layer* rules these correlation functions will be written as sum over different diagrams of  $\mathcal{C}_{n,lc}(\mathcal{G}; \{\mathcal{L}\})$  the  $n$ -point line-connected correlation, averaged over the realizations of the percolation problem and computed on the diagram  $\mathcal{G}$  embedded on a tree graph, where  $\{\mathcal{L}\}$  indicates the length of the different lines entering the diagram. The two-point (three-point) correlation is defined as the probability that two (three) sites, at positions  $x_1$  and  $x_2$  ( $x_1, x_2$  and  $x_3$ ) are occupied and belong to the same cluster. In the end, at one loop level, we must subtract pieces already considered in loop-free diagrams, to compute the “line-connected” observable [12, 24]. We analyse the two observables separately, following for each of them the steps listed in the previous section.

### Observable: $\overline{C_2(x_1, x_2)}$

- Step 1: *Identify the possible topological diagrams*

The simplest diagram connecting two points is the bare line, which we will call  $\mathcal{G}_1$ . Including the possibility of a loop to be present we consider the diagram composed of four



lines with two vertices of degree three, where the two internal lines compose a loop. We will call this diagram  $\mathcal{G}_2$ .

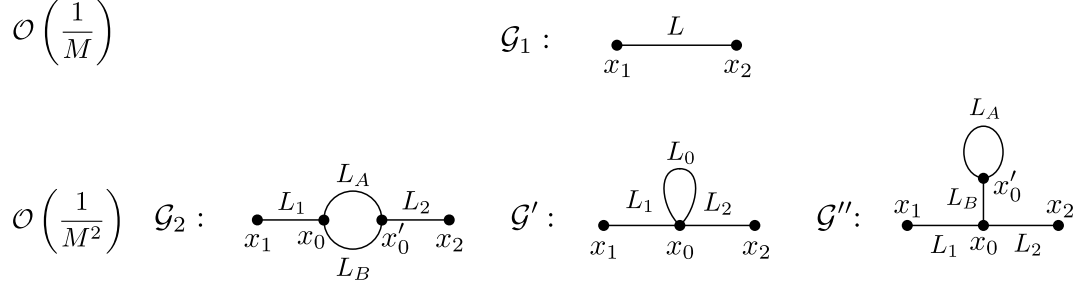


Figure 1: Diagrams that contribute to the two-point correlation functions up to one loop.

Other possibilities are the tadpole-type diagrams, connecting two points with a loop generated by one four-degree vertex or connecting two points by two three-degree vertices, respectively the diagrams  $\mathcal{G}'$  and  $\mathcal{G}''$  in Fig. 1. Nevertheless, these last two diagrams give no contributions to the *line-connected* two-point observable for percolation, as we will see in Step 3 below. We won't consider them in the following steps.

- Step 2: *Weights, number of projections and symmetry factors*

Diagram  $\mathcal{G}_1$ :

- ◆  $W(\mathcal{G}_1) = \frac{1}{M}$ ;
- ◆  $\mathcal{N}(\mathcal{G}_1; L; x_1, x_2) = (2D)^2 \mathcal{N}_L(x_1, x_2)$ ;
- ◆  $S(\mathcal{G}_1) = 1$ .

Diagram  $\mathcal{G}_2$ :

- ◆  $W(\mathcal{G}_2) = \frac{1}{M^2}$ ;
- ◆  $\mathcal{N}(\mathcal{G}_2; \vec{L}; x_1, x_2) = (2D)^2 \left( \frac{(2D)!}{(2D-3)!} \right)^2 \sum_{x_0, x'_0} \mathcal{N}_{L_1}(x_1, x_0) \mathcal{N}_{L_A}(x_0, x'_0) \mathcal{N}_{L_B}(x_0, x'_0) \mathcal{N}_{L_2}(x'_0, x_2)$ ;
- ◆  $S(\mathcal{G}_2) = 2$ .

where  $\vec{L} = (L_1, L_A, L_B, L_2)$ .

- Step 3: *Computation of  $\mathcal{C}_{2,lc}(\mathcal{G}_1; L)$  and  $\mathcal{C}_{2,lc}(\mathcal{G}_2; \vec{L})$*

Given the definition of the line-connected two-point correlation for the site percolation problem, we compute the two contributions:

$$\mathcal{C}_{2,lc}(\mathcal{G}_1; L) = p p^L; \quad (33)$$

$$\mathcal{C}_{2,lc}(\mathcal{G}_2; \vec{L}) = -p^{L_1+L_2+L_A+L_B}. \quad (34)$$

The first result is immediate since, in the non-percolating phase, all the  $L + 1$  sites, connected by a line of length  $L$ , must be active, in order to connect the two sites at the extremities. The second result appears because, for the sites at the extremities to be connected, one or both lines of the loop must consist of active sites, in addition to the external lines, which also need to be composed of active sites. The associated probability for this to happen is  $p^{L_1+1}(p^{L_A-1} + p^{L_B-1} - p^{L_A+L_B-2})p^{L_2+1}$ . The aforementioned result is obtained subtracting the straight line contributions, already taken into account with  $\mathcal{G}_1$ :  $p^{L_1+1}p^{L_A-1}p^{L_2+1}$  and  $p^{L_1+1}p^{L_B-1}p^{L_2+1}$ . This last operation is the application of the “line-connected” definition [12].

Performing the same computation for diagrams  $\mathcal{G}'$  and  $\mathcal{G}''$  we obtain zero, as anticipated. The reason is that the two tadpoles, that enter the site  $x_0$ , do not change the probability that sites  $x_1$  and  $x_2$  belong to the same cluster with respect to case where the loop is not present. Indeed, independently of the lines of the tadpole, site  $x_0$  must be active in order to connect the two sites, then, subtracting the contributions needed to define the line-connected observable, that are the simple lines without tadpoles, the net contribution is zero. These diagrams are instead relevant in the percolating phase that we aim to study in a subsequent work.

- Step 4: *Sum of the contributions*

$$\begin{aligned} \overline{C_2(x_1, x_2)} &= \frac{1}{M} \sum_L \mathcal{N}(\mathcal{G}_1; L; x_1, x_2) \mathcal{C}_{2,lc}(\mathcal{G}_1; L) + \\ &+ \frac{1}{2M^2} \sum_{\vec{L}} \mathcal{N}(\mathcal{G}_2; \vec{L}; x_1, x_2) \mathcal{C}_{2,lc}(\mathcal{G}_2; \vec{L}) + \mathcal{O}\left(\frac{1}{M^3}\right). \end{aligned} \quad (35)$$

**Observable:**  $\overline{C_3(x_1, x_2, x_3)}$

- Step 1: *Identify the possible topological diagrams*

The simplest diagram connecting three points is the bare three-degree vertex, which we will call  $\mathcal{G}_3$ . Including the possibility for a loop to be present, we consider the diagram, composed by six lines, with three three-degree vertices, where the three internal lines compose a loop; We will call this diagram  $\mathcal{G}_4$ . At one-loop level there are three more diagrams connecting three points with a single loop, which are the same as  $\mathcal{G}_3$ , but one of the external legs is dressed with  $\mathcal{G}_2$ . We call such a diagram  $\mathcal{G}_5$ , including all the permutations. All these diagrams are reported in Fig. 2.

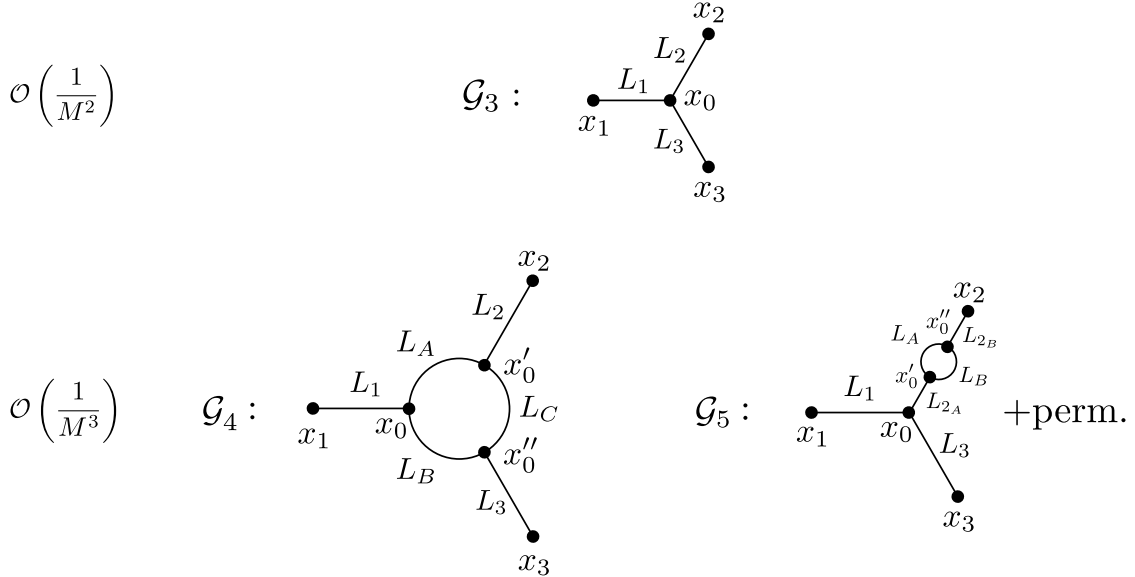


Figure 2: Diagrams that contribute to the three-point correlation functions up to one loop.

- Step 2: *Weights, number of projections and symmetry factors*

Diagram  $\mathcal{G}_3$ :

- ◆  $W(\mathcal{G}_3) = \frac{1}{M^2}$ ;
- ◆  $\mathcal{N}(\mathcal{G}_3; \vec{L}; x_1, x_2, x_3) = (2D)^3 \frac{(2D)!}{(2D-3)!} \sum_{x_0} \prod_{i=1}^3 \mathcal{N}_{L_i}(x_i, x_0)$ ;

$$\blacklozenge S(\mathcal{G}_3) = 1.$$

Diagram  $\mathcal{G}_4$ :

$$\blacklozenge W(\mathcal{G}_4) = \frac{1}{M^3};$$

$$\begin{aligned} \blacklozenge \mathcal{N}(\mathcal{G}_4; \vec{L}''; x_1, x_2, x_3) &= \\ &= (2D)^3 \left( \frac{(2D)!}{(2D-3)!} \right)^3 \times \\ &\quad \sum_{x_0, x'_0, x''_0} \mathcal{N}_{L_1}(x_1, x_0) \mathcal{N}_{L_2}(x_2, x'_0) \mathcal{N}_{L_3}(x_3, x''_0) \mathcal{N}_{L_A}(x_0, x'_0) \mathcal{N}_{L_B}(x_0, x''_0) \mathcal{N}_{L_C}(x'_0, x''_0); \end{aligned}$$

$$\blacklozenge S(\mathcal{G}_4) = 1.$$

Diagram  $\mathcal{G}_5$ :

$$\blacklozenge W(\mathcal{G}_5) = \frac{1}{M^3};$$

$$\begin{aligned} \blacklozenge \mathcal{N}(\mathcal{G}_5; \vec{L}'''; x_1, x_2, x_3) &= \\ &= (2D)^3 \left( \frac{(2D)!}{(2D-3)!} \right)^3 \times \\ &\quad \sum_{x_0, x'_0, x''_0} \mathcal{N}_{L_1}(x_1, x_0) \mathcal{N}_{L_{2A}}(x_0, x'_0) \mathcal{N}_{L_A}(x'_0, x''_0) \mathcal{N}_{L_B}(x''_0, x'_0) \mathcal{N}_{L_{2B}}(x_2, x''_0) \mathcal{N}_{L_3}(x_3, x_0); \end{aligned}$$

$$\blacklozenge S(\mathcal{G}_5) = 2,$$

where  $\vec{L}' = (L_1, L_2, L_3)$ ,  $\vec{L}'' = (\vec{L}', L_A, L_B, L_C)$  and  $\vec{L}''' = (L_1, L_{2A}, L_A, L_B, L_{2B}, L_3)$ .

- Step 3: *Computation of  $\mathcal{C}_{3,lc}(\mathcal{G}_3; \vec{L}')$ ,  $\mathcal{C}_{3,lc}(\mathcal{G}_4; \vec{L}'')$  and  $\mathcal{C}_{3,lc}(\mathcal{G}_5; \vec{L}''')$*

As for the two-point function we compute the two contributions:

$$\mathcal{C}_{3,lc}(\mathcal{G}_3; \vec{L}') = p p^{L_1+L_2+L_3}; \quad (36)$$

$$\mathcal{C}_{3,lc}(\mathcal{G}_4; \vec{L}'') = -2p^{L_1+L_2+L_3+L_A+L_B+L_C}; \quad (37)$$

$$\mathcal{C}_{3,lc}(\mathcal{G}_5; \vec{L}''') = -p^{L_1+L_{2A}+L_{2B}+L_A+L_B+L_3}. \quad (38)$$

The result for  $\mathcal{G}_3$  is easily derived, considering that all the sites of the topology must be active for the extremities to be connected. The result for  $\mathcal{G}_5$  is obtained multiplying the contribution for the bare vertex and the loop correction of the two-point function, diagram  $\mathcal{G}_2$ , with the corresponding lengths. The contribution of  $\mathcal{G}_4$  is a generalization of the computation for  $\mathcal{G}_2$ ; to connect the three extremities two of the three (or all the three) lines of the loop must consist on all active sites. Moreover, in this case we have to subtract three contributions, corresponding to cutting  $L_A$ ,  $L_B$ , and  $L_C$  respectively, already included in the bare contribution  $\mathcal{G}_3$ .

- Step 4: *Sum of the contributions*

$$\begin{aligned} \overline{C_3(x_1, x_2, x_3)} &= \frac{1}{M^2} \sum_{\vec{L}'} \mathcal{N}(\mathcal{G}_3; \vec{L}'; x_1, x_2, x_3) \mathcal{C}_{3,lc}(\mathcal{G}_3; \vec{L}') + \\ &\quad + \frac{1}{M^3} \sum_{\vec{L}''} \mathcal{N}(\mathcal{G}_4; \vec{L}''; x_1, x_2, x_3) \mathcal{C}_{3,lc}(\mathcal{G}_4; \vec{L}'') + \\ &\quad + \frac{1}{2M^3} \sum_{\vec{L}'''} \mathcal{N}(\mathcal{G}_5; \vec{L}'''; x_1, x_2, x_3) \mathcal{C}_{3,lc}(\mathcal{G}_5; \vec{L}''') + \mathcal{O}\left(\frac{1}{M^4}\right). \end{aligned} \quad (39)$$

In appendix C we discuss why we didn't include other possible but *irrelevant* diagrams to study the critical behavior of the percolation problem and we present the explicit computation of the leading order critical behaviour of the four-point correlation function.

**Computation of the moments of  $n(\mathbf{s}, \mathbf{p})$**  In order to compute  $\chi_2$  and  $\chi_3$  we Fourier transform  $\overline{C_2(x_1, x_2)}$  and  $\overline{C_3(x_1, x_2, x_3)}$ , given in Eqs. (35) and (39), using the following convention:

$$\widehat{h}(k) = a_l^D \sum_{x \in a_l \mathbb{Z}^D} h(x) e^{ikx}, \quad h(x) = \int_{[-\frac{\pi}{a_l}, \frac{\pi}{a_l}]} \frac{d^D k}{(2\pi)^D} \widehat{h}(k) e^{-ikx}; \quad (40)$$

that imply

$$\left(\frac{2\pi}{a_l}\right)^D \delta^D(k) = \sum_{x \in a_l \mathbb{Z}^D} e^{ikx}. \quad (41)$$

We also use the fact that  $\mathcal{N}_L(x_1, x_2)$  is a function of the difference between the starting and arrival point only, so that, in Fourier space, we have

$$\widehat{\mathcal{N}}_L(k_1, k_2) = (2\pi)^D \delta(k_1 + k_2) \widehat{\mathcal{N}}_L(k_1) \quad (42)$$

where, for small  $k$  [12, 15],

$$\widehat{\mathcal{N}}_L(k) \approx 2D(2D-1)^{L-1} a_l^D e^{-k^2 a_l^2 L/(2D-2)}. \quad (43)$$

In view of the fact that in the critical region the sums will be dominated by large  $L$  contributions, we may write the sums over the lengths as integrals:

$$\sum_{L=1}^{\infty} \rightarrow \int_{1/\Lambda^2}^{\infty} dL, \quad (44)$$

where we introduced the UV cutoff  $\Lambda = 1$  to make contact with field theory. Note that while in field-theory the UV cutoff is inserted manually, in the  $M$ -layer construction it arises naturally due to the lattice spacing (see more details in the appendix B). The resulting expressions for the two and three-point functions are respectively

$$\begin{aligned} \overline{\widehat{C}_2(k, k')} &= \frac{\widehat{C} \widehat{B}^2 a_l^D}{\widehat{A} \mu} \frac{1}{\widehat{k}^2 + 1} (2\pi)^D \delta^D(k + k') \times \\ &\times \left( 1 - \frac{\widehat{A} \mu^{\frac{D}{2}-3}}{2(\widehat{k}^2 + 1)} \int \frac{d^D \widehat{q}}{(2\pi)^D} \int d\widehat{L}_A d\widehat{L}_B e^{-(1+(\widehat{k}-\widehat{q})^2)\widehat{L}_A} e^{-(1+\widehat{q}^2)\widehat{L}_B} \right) + \mathcal{O}\left(\frac{1}{M^3}\right) \end{aligned} \quad (45)$$

and

$$\begin{aligned} \overline{\widehat{C}_3(k_1, k_2, k_3)} &= \frac{\widehat{C} \widehat{B}^3 a_l^{2D}}{\widehat{A} \mu^3} \frac{(2\pi)^D \delta^D(k_1 + k_2 + k_3)}{(\widehat{k}_1^2 + 1)(\widehat{k}_2^2 + 1)(\widehat{k}_3^2 + 1)} \times \\ &\left( 1 - 2\widehat{A} \mu^{\frac{D}{2}-3} \int \frac{d^D \widehat{q}}{(2\pi)^D} \int d\widehat{L}_A d\widehat{L}_B d\widehat{L}_C e^{-(1+(\widehat{k}_2+\widehat{k}_3+\widehat{q})^2)\widehat{L}_A} e^{-(1+(\widehat{k}_2+\widehat{q})^2)\widehat{L}_B} e^{-(1+\widehat{q}^2)\widehat{L}_C} + \right. \\ &\left. - \frac{1}{2} \frac{\widehat{A} \mu^{\frac{D}{2}-3}}{(\widehat{k}_2 + \widehat{k}_3)^2 + 1} \int \frac{d^D \widehat{q}}{(2\pi)^D} \int d\widehat{L}_A d\widehat{L}_B e^{-(1+(\widehat{k}_2+\widehat{q})^2)\widehat{L}_A} e^{-(1+\widehat{q}^2)\widehat{L}_B} + perm. \right) + \mathcal{O}\left(\frac{1}{M^4}\right), \end{aligned} \quad (46)$$

where  $\mu$  is the one defined in Eq. (32) and we also defined the following non-universal constants:

$$\widehat{A} \equiv \frac{1}{M} \left( \frac{(2D)!}{(2D-3)!} \right)^2 p^{-1} (2D-2)^{\frac{D}{2}} \left( \frac{2D}{2D-1} \right)^3, \quad (47)$$

$$\widehat{B} \equiv \frac{1}{M} 2D \left( \frac{(2D)!}{(2D-3)!} \right) \left( \frac{2D}{2D-1} \right)^2, \quad (48)$$

$$\widehat{C} \equiv (2D-2)^{\frac{D}{2}}, \quad (49)$$

and we rescaled the momenta and lengths according to:

$$\widehat{k} \equiv k \frac{a_l}{\sqrt{\mu(2D-2)}}, \quad \text{and} \quad \widehat{L}_i \equiv L_i \mu. \quad (50)$$

Note that in Eqs. (45), (46) we have omitted the the extremes of integration  $(\mu/\Lambda^2, \infty)$  of the integrals over  $\widehat{L}$ . In appendix A we show how to generalize this kind of computation for a  $V_e$ -point function, with  $V_e \geq 2$ , moreover we explain the reasoning behind the identification of the constants  $\widehat{A}$ ,  $\widehat{B}$  and  $\widehat{C}$ . In appendix B we show that the above expression, for  $\widehat{C}_2(k, k')$  and  $\widehat{C}_3(k_1, k_2, k_3)$ , are precisely the same that appear from the Feynman diagrams of the corresponding scalar cubic field-theory obtained from the Fortuin-Kasteleyn mapping to the  $n+1$ -state Potts model in the limit  $n \rightarrow 0$ , corresponding to percolation [6–9].

From the above expressions we compute the functions  $\chi_q$  introduced in section 2. Notice that we did not rescale the momenta inside the momentum conservation delta functions, thus, to compute  $\chi_q$ , according to Eq. (6), we have simply to divide by  $a_l^{(q-1)D}$ , remove  $(2\pi)^D$  times the conservation delta function and set the external momenta to zero. This leads to

$$\chi_2(\mu) = \frac{\widehat{C}\widehat{B}^2}{\widehat{A}\mu} \left( 1 - \frac{\widehat{A}\mu^{\frac{D}{2}-3}}{2(4\pi)^{\frac{D}{2}}} \int \frac{d\widehat{L}_A d\widehat{L}_B}{(\widehat{L}_A + \widehat{L}_B)^{\frac{D}{2}}} e^{-\widehat{L}_A - \widehat{L}_B} \right), \quad (51)$$

$$\begin{aligned} \chi_3(\mu) = \frac{\widehat{C}\widehat{B}^3}{\widehat{A}\mu^3} & \left( 1 - \frac{2\widehat{A}\mu^{\frac{D}{2}-3}}{(4\pi)^{\frac{D}{2}}} \int \frac{d\widehat{L}_A d\widehat{L}_B d\widehat{L}_C}{(\widehat{L}_A + \widehat{L}_B + \widehat{L}_C)^{\frac{D}{2}}} e^{-\widehat{L}_A - \widehat{L}_B - \widehat{L}_C} + \right. \\ & \left. - \frac{3}{2} \widehat{A}\mu^{\frac{D}{2}-3} \int \frac{d\widehat{L}_A d\widehat{L}_B}{(\widehat{L}_A + \widehat{L}_B)^{\frac{D}{2}}} e^{-\widehat{L}_A - \widehat{L}_B} \right). \end{aligned} \quad (52)$$

Introducing the function  $\widehat{G}(k)$ , corresponding to the *propagator* in the field-theoretical language, as

$$\overline{\widehat{C}_2(k, k')} \equiv (2\pi)^D \delta^D(k + k') \widehat{G}(k), \quad (53)$$

we can define the correlation length  $\xi$ :

$$\xi^2 \equiv \widehat{G}(0) \frac{\partial \widehat{G}^{-1}(k)}{\partial k^2} \Big|_{k^2=0} \quad (54)$$

where with a little abuse of notation we identify with  $k$  the modulus of the corresponding vector. Since

$$\frac{\partial}{\partial k^2} = \frac{\partial \widehat{k}^2}{\partial k^2} \frac{\partial}{\partial \widehat{k}^2} = \frac{a_l^2}{\mu \widehat{C}^{\frac{2}{D}}} \frac{\partial}{\partial \widehat{k}^2} \quad (55)$$

we have:

$$\widehat{G}(0) = \frac{\widehat{C}\widehat{B}^2 a_l^D}{\widehat{A}\mu} \left( 1 - \frac{\widehat{A}\mu^{\frac{D}{2}-3}}{2(4\pi)^{\frac{D}{2}}} \int \frac{d\widehat{L}_A d\widehat{L}_B}{(\widehat{L}_A + \widehat{L}_B)^{\frac{D}{2}}} e^{-\widehat{L}_A - \widehat{L}_B} \right), \quad (56)$$

and for small  $k$ :

$$\widehat{G}^{-1}(k) \simeq \frac{\widehat{A}\mu}{\widehat{C}\widehat{B}^2 a_l^D} \left( \widehat{k}^2 + 1 + \frac{\widehat{A}\mu^{\frac{D}{2}-3}}{2(4\pi)^{\frac{D}{2}}} \int \frac{d\widehat{L}_a d\widehat{L}_b}{(\widehat{L}_a + \widehat{L}_b)^{\frac{D}{2}}} e^{-\frac{\widehat{L}_a \widehat{L}_b}{\widehat{L}_a + \widehat{L}_b} \widehat{k}^2 - \widehat{L}_a - \widehat{L}_b} \right), \quad (57)$$

from which:

$$\left. \frac{\partial \widehat{G}^{-1}(k)}{\partial \widehat{k}^2} \right|_{\widehat{k}^2=0} = \frac{\widehat{A}\mu}{\widehat{C}\widehat{B}^2 a_l^D} \left( 1 + \frac{\widehat{A}\mu^{\frac{D}{2}-3}}{2(4\pi)^{\frac{D}{2}}} \int \frac{d\widehat{L}_a d\widehat{L}_b}{(\widehat{L}_a + \widehat{L}_b)^{\frac{D}{2}}} e^{-\widehat{L}_a - \widehat{L}_b} \frac{\partial}{\partial \widehat{k}^2} \left( e^{-\frac{\widehat{L}_a \widehat{L}_b}{\widehat{L}_a + \widehat{L}_b} \widehat{k}^2} \right) \right|_{\widehat{k}^2=0} \right), \quad (58)$$

where

$$\int \frac{d\widehat{L}_a d\widehat{L}_b}{(\widehat{L}_a + \widehat{L}_b)^{\frac{D}{2}}} e^{-\widehat{L}_a - \widehat{L}_b} \frac{\partial}{\partial \widehat{k}^2} \left( e^{-\frac{\widehat{L}_a \widehat{L}_b}{\widehat{L}_a + \widehat{L}_b} \widehat{k}^2} \right) \Big|_{\widehat{k}^2=0} = - \int \frac{d\widehat{L}_a d\widehat{L}_b}{(\widehat{L}_a + \widehat{L}_b)^{\frac{D}{2}+1}} \widehat{L}_A \widehat{L}_B e^{-\widehat{L}_a - \widehat{L}_b}. \quad (59)$$

Defining

$$I_\alpha(\mu) \equiv \int_{\mu/\Lambda^2}^{\infty} d\widehat{L}_a d\widehat{L}_b \frac{e^{-\widehat{L}_a - \widehat{L}_b}}{(\widehat{L}_a + \widehat{L}_b)^{\frac{D}{2}}} \quad (60)$$

and

$$I_\beta(\mu) \equiv \int_{\mu/\Lambda^2}^{\infty} d\widehat{L}_a d\widehat{L}_b \frac{\widehat{L}_a \widehat{L}_b}{(\widehat{L}_a + \widehat{L}_b)^{\frac{D}{2}+1}} e^{-\widehat{L}_a - \widehat{L}_b}, \quad (61)$$

we have

$$\xi^2(\mu) = \frac{1}{m^2(\mu)} = \frac{a_l^2}{\widehat{C}^{\frac{2}{D}} \mu} \left( 1 - \frac{1}{2} \frac{\widehat{A}\mu^{\frac{D}{2}-3}}{(4\pi)^{\frac{D}{2}}} \left( I_\alpha(\mu) + I_\beta(\mu) \right) \right). \quad (62)$$

In the integrals in Eqs. (60), (61), we have written explicitly the extremes of integration that we have omitted in the precedent integrals. Notice that the integral  $I_\alpha(\mu)$  is divergent in  $D = 6$  for  $\mu \rightarrow 0$  (i.e.,  $p \rightarrow p_c$ ).

Now we can simply invert the relation, to express  $\mu$  as a function of  $m^2$ :

$$\mu(m^2) = a_l^2 \widehat{C}^{-\frac{2}{D}} m^2 \left( 1 - \frac{1}{2} \frac{\widehat{A} m^{D-6} \widehat{C}^{\frac{6}{D}-1} a_l^{D-6}}{(4\pi)^{\frac{D}{2}}} \left( I_\alpha(\mu(m^2)) + I_\beta(\mu(m^2)) \right) \right). \quad (63)$$

Notice that the previous Eqs. for  $\chi_2$  and  $\chi_3$  are written as functions of  $\mu$ , which is not the “physical mass”, thus they can be divergent, for  $\mu \rightarrow 0$ , near the upper critical dimension,  $D_U = 6$ . To avoid the divergences we need the expression of  $\mu$  as a function of  $m^2$ , to correctly write  $\lambda$ , as defined in Eq. (67). To this aim we compute  $\xi^2(\mu)$  (and so  $m^2(\mu)$ ) from its definition.

At this point we have all the ingredients to write  $\chi_2$  and  $\chi_3$  as functions of the physical parameter  $m^2$ . Plugging Eq. (63) into Eqs. (51) and (52) we obtain:

$$\begin{aligned} \chi_2(m^2) &= \frac{\widehat{C}\widehat{B}^2 \widehat{C}^{\frac{2}{D}}}{\widehat{A} a_l^2} m^{-2} \left( 1 + \frac{1}{2} \frac{\widehat{A} m^{D-6} \widehat{C}^{\frac{6}{D}-1} a_l^{D-6}}{(4\pi)^{\frac{D}{2}}} \left( I_\alpha(\mu(m^2)) + I_\beta(\mu(m^2)) \right) \right) \times \\ &\quad \times \left( 1 - \frac{1}{2} \frac{\widehat{A} m^{D-6} \widehat{C}^{\frac{6}{D}-1} a_l^{D-6}}{(4\pi)^{\frac{D}{2}}} I_\alpha(\mu(m^2)) \right) = \\ &= \frac{\widehat{C}\widehat{B}^2 \widehat{C}^{\frac{2}{D}}}{\widehat{A} a_l^2} m^{-2} \left( 1 + \frac{1}{2} \frac{\widehat{A} m^{D-6} \widehat{C}^{\frac{6}{D}-1} a_l^{D-6}}{(4\pi)^{\frac{D}{2}}} I_\beta(\mu(m^2)) \right), \end{aligned} \quad (64)$$

$$\begin{aligned}
 \chi_3(m^2) &= \frac{\widehat{C}\widehat{B}^3\widehat{C}^{\frac{6}{D}}}{\widehat{A}a_l^6} m^{-6} \left( 1 + \frac{3}{2} \frac{\widehat{A}m^{D-6}\widehat{C}^{\frac{6}{D}-1}a_l^{D-6}}{(4\pi)^{\frac{D}{2}}} \left( I_\alpha(\mu(m^2)) + I_\beta(\mu(m^2)) \right) \right) \times \\
 &\quad \times \left( 1 - 2 \frac{\widehat{A}m^{D-6}\widehat{C}^{\frac{6}{D}-1}a_l^{D-6}}{(4\pi)^{\frac{D}{2}}} I_\gamma(\mu(m^2)) - \frac{3}{2} \frac{\widehat{A}m^{D-6}\widehat{C}^{\frac{6}{D}-1}a_l^{D-6}}{(4\pi)^{\frac{D}{2}}} I_\alpha(\mu(m^2)) \right) \\
 &= \frac{\widehat{C}\widehat{B}^3\widehat{C}^{\frac{6}{D}}}{\widehat{A}a_l^6} m^{-6} \left( 1 + \frac{\widehat{A}m^{D-6}\widehat{C}^{\frac{6}{D}-1}a_l^{D-6}}{(4\pi)^{\frac{D}{2}}} \left( \frac{3}{2} I_\beta(\mu(m^2)) - 2I_\gamma(\mu(m^2)) \right) \right), \quad (65)
 \end{aligned}$$

where

$$I_\gamma(\mu) \equiv \int_{\mu/\Lambda^2}^{\infty} d\widehat{L}_A d\widehat{L}_B d\widehat{L}_C \frac{e^{-\widehat{L}_A - \widehat{L}_B - \widehat{L}_C}}{(\widehat{L}_A + \widehat{L}_B + \widehat{L}_C)^{\frac{D}{2}}}. \quad (66)$$

Notice that  $\chi_2(\mu)$  and  $\chi_3(\mu)$  have UV divergences near 6 dimensions due the presence of  $I_\alpha(\mu)$ , while  $I_\alpha(\mu)$  disappears when they are written as functions of  $m$ , *i.e.*  $\chi_2(m^2)$  and  $\chi_3(m^2)$  are free of UV divergences near 6 dimensions.

**Critical exponents in fixed dimension** In this section we perform the fixed-dimension computation of the critical exponents [20]. Led by the scaling laws discussed in sec. 2, we compute the following adimensional ratio:

$$\lambda \equiv \left( \frac{a_l}{\xi} \right)^D \frac{\chi_3^2(m^2)}{\chi_2^3(m^2)}, \quad (67)$$

On the other end  $m^2$  is connected to the bare distance from the critical point by

$$m^2 \sim (\mu - \mu_c)^{2\nu} \quad \text{and} \quad \xi \sim (\mu - \mu_c)^{-\nu}, \quad (68)$$

where  $\nu$  is the critical exponent for the divergence of the correlation length.

In the end, defining

$$u \equiv \widehat{A}\widehat{C}^{\frac{6}{D}-1}a_l^{D-6} m^{D-6} \equiv g m^{D-6}, \quad (69)$$

we can compute the ratio  $\lambda$

$$\lambda = u \left( 1 - 2 \frac{u}{(4\pi)^{\frac{D}{2}}} \left( -\frac{3}{4} I_\beta(\mu(m^2)) + 2I_\gamma(\mu(m^2)) \right) \right). \quad (70)$$

Note that  $\lambda$  depends on the microscopic parameter of the model only through the single parameter  $u = O(1/M)$ . Now we can compute the integrals  $I_\beta$  and  $I_\gamma$  in the limit  $m^2 \rightarrow 0$ , which are convergent near  $D = 6$ :

$$\lim_{m^2 \rightarrow 0} I_\beta(\mu(m^2)) = \frac{1}{6} \Gamma \left( 3 - \frac{D}{2} \right), \quad (71)$$

$$\lim_{m^2 \rightarrow 0} I_\gamma(\mu(m^2)) = \frac{1}{2} \Gamma \left( 3 - \frac{D}{2} \right). \quad (72)$$

Thus in the limit  $m^2 \rightarrow 0$

$$\lambda = u - \frac{7}{4} \frac{u^2}{(4\pi)^{\frac{D}{2}}} \Gamma \left( 3 - \frac{D}{2} \right), \quad (73)$$

from which

$$u \simeq \lambda + \frac{7}{4} \frac{\lambda^2}{(4\pi)^{\frac{D}{2}}} \Gamma\left(3 - \frac{D}{2}\right). \quad (74)$$

Now, following the standard procedure (see ref. [20], chap. 8), we define the function  $b(\lambda)$  as:

$$b(\lambda) \equiv m^2 \frac{\partial}{\partial m^2} \bigg|_{g \text{ fixed}} \lambda = \frac{1}{2}(D-6)u \frac{\partial}{\partial u} \bigg|_{m^2 \text{ fixed}} \lambda = \frac{1}{2}(D-6) \left( u - \frac{7}{2} \frac{u^2}{(4\pi)^{\frac{D}{2}}} \Gamma\left(3 - \frac{D}{2}\right) \right). \quad (75)$$

From Eq. (74) we obtain:

$$b(\lambda) = \frac{1}{2}(D-6) \left( \lambda - \frac{7}{4} \frac{\lambda^2}{(4\pi)^{\frac{D}{2}}} \Gamma\left(3 - \frac{D}{2}\right) \right). \quad (76)$$

We constructed  $\lambda$  to be an adimensional quantity that does not diverge at the critical point. For this reason, we can identify the critical value of  $\lambda$  as the point at which the function  $b(\lambda)$  is zero, as we discussed in section (2). While a trivial zero is always present at  $\lambda = 0$ , for  $D < 6$  we see that there also exists a non-trivial zero:

$$\lambda_c = \frac{4}{7} \frac{(4\pi)^{\frac{D}{2}}}{\Gamma\left(3 - \frac{D}{2}\right)}. \quad (77)$$

Remembering that  $m^2 \sim (\mu - \mu_c)^{2\nu}$ , following standard computations [20], we define:

$$z(\lambda) \equiv \frac{\partial \mu}{\partial m^2} \propto m^{2D_1}, \quad (78)$$

where  $D_1 = \frac{1}{2\nu} - 1$ . We can thus compute it as:

$$D_1(\lambda) \equiv m^2 \frac{\partial}{\partial m^2} \bigg|_{g \text{ fixed}} \ln(z(\lambda)). \quad (79)$$

In the same way, for the computation of  $\eta$  we need to define:

$$D_2(\lambda) \equiv \frac{\partial \ln \chi_2(0)}{\partial \ln m^2} \bigg|_{g \text{ fixed}}, \quad \chi_2(0) \propto m^{2\frac{\eta-2}{2}}, \quad D_2(\lambda_c) = -1 + \frac{\eta}{2}. \quad (80)$$

We start from the computation of  $z$ :

$$z(\lambda) = a_l^2 \hat{C}^{-\frac{2}{D}} \left( 1 - \frac{1}{2} \frac{u}{(4\pi)^{\frac{D}{2}}} \frac{D-4}{2} I_\beta(\mu(m^2)) - \frac{1}{2} \frac{g}{(4\pi)^{\frac{D}{2}}} \frac{\partial}{\partial m^2} \left( m^{D-4} I_\alpha(\mu(m^2)) \right) \right) \quad (81)$$

where

$$\frac{\partial}{\partial m^2} \left( m^{D-4} I_\alpha(\mu(m^2)) \right) = -m^{D-6} \int_{\mu(m^2)/\Lambda^2}^{\infty} d\hat{L}_a d\hat{L}_b \frac{e^{-\hat{L}_a - \hat{L}_b}}{(\hat{L}_a + \hat{L}_b)^{\frac{D}{2}-1}} \equiv -m^{D-6} I'_\alpha(\mu(m^2)). \quad (82)$$

We can compute  $I'_\alpha$ :

$$\lim_{m^2 \rightarrow 0} I'_\alpha(\mu(m^2)) = \Gamma\left(3 - \frac{D}{2}\right), \quad (83)$$



obtaining

$$z(\lambda) \propto 1 - \frac{u}{2} \frac{1}{(4\pi)^{\frac{D}{2}}} \Gamma\left(3 - \frac{D}{2}\right) \frac{D-16}{12}, \quad (84)$$

and, from the definition of  $D_1(\lambda)$  we arrive at the critical exponent  $\nu$  in  $D$  dimensions:

$$\nu_D = \frac{42}{84 + (6-D)(D-16)}. \quad (85)$$

The next exponent,  $\eta$ , requires the computation of  $D_2(\lambda)$

$$D_2(\lambda) \equiv \left. \frac{\partial \ln \chi_2}{\partial \ln m^2} \right|_{g \text{ fixed}} = \frac{m^2}{\chi_2} \left. \frac{\partial \chi_2}{\partial m^2} \right|_{g \text{ fixed}} = -1 + \frac{\lambda}{2} \frac{1}{(4\pi)^{\frac{D}{2}}} I_\beta(\mu(m^2)) \left( \frac{D}{2} - 3 \right), \quad (86)$$

which can be obtained using

$$\left. \frac{\partial \chi_2}{\partial m^2} \right|_{g \text{ fixed}} \propto -m^{-4} + \frac{1}{2} \frac{u}{(4\pi)^{\frac{D}{2}}} m^{-4} I_\beta(\mu(m^2)) \frac{D-8}{2} = -m^{-4} \left( 1 - \frac{1}{2} \frac{u}{(4\pi)^{\frac{D}{2}}} I_\beta(\mu(m^2)) \frac{D-8}{2} \right), \quad (87)$$

$$\chi_2 \propto m^{-2} \left( 1 + \frac{1}{2} \frac{u}{(4\pi)^{\frac{D}{2}}} I_\beta(\mu(m^2)) \right), \quad (88)$$

from which we have

$$\eta_D = \frac{D-6}{21}. \quad (89)$$

**$\epsilon$ -expansion** Given the results of Eqs. (85) and (89) in fixed dimension we can perform the computation in  $D = 6 - \epsilon$ :

$$\nu = \frac{1}{2} + \frac{5}{84} \epsilon + \mathcal{O}(\epsilon^2), \quad (90)$$

$$\eta = -\frac{1}{21} \epsilon + \mathcal{O}(\epsilon^2). \quad (91)$$

These results are, to first order in  $\epsilon$ , equal to the expansion of the standard field theory associated with the percolation problem [3, 6, 8–11].

## 6 The case of bond percolation

An interesting application of the  $M$ -layer construction to percolation theory is to show that there is no difference between the critical behavior of the site and the bond percolation problems. Standard field theoretical approaches are used to compute the critical exponents, resorting to the mapping between the  $(n+1)$ -state Potts model and the bond percolation in the limit  $n \rightarrow 0$  [25]. Here we show how to apply the same procedure described in the previous section to the bond percolation. The bond percolation is defined as the site one, with the only difference that now  $p$  is the probability that each bond independently is present. Thus, the only differences are the computations of  $\mathcal{C}_{2,lc}(\mathcal{G}; \{\vec{\mathcal{L}}\})$  and  $\mathcal{C}_{3,lc}(\mathcal{G}; \{\vec{\mathcal{L}}\})$  on the different diagrams mentioned in Sec. 5, that for bond percolation take the form:

$$\mathcal{C}_{2,lc}^{bond}(\mathcal{G}_1; L) = p^L; \quad (92)$$

$$\mathcal{C}_{2,lc}^{bond}(\mathcal{G}_2; \vec{L}) = -p^{L_1+L_2+L_A+L_B}; \quad (93)$$

$$\mathcal{C}_{3,lc}^{bond}(\mathcal{G}_3; \vec{L}') = p^{L_1+L_2+L_3}; \quad (94)$$

$$\mathcal{C}_{3,lc}^{bond}(\mathcal{G}_4; \vec{L}'') = -2p^{L_1+L_2+L_3+L_A+L_B+L_C}; \quad (95)$$

$$\mathcal{C}_{3,lc}^{bond}(\mathcal{G}_5; \vec{L}''') = -p^{L_1+L_2+L_3+L_A+L_B+L_C}. \quad (96)$$

As one can see, the expressions of the observables in the Bethe lattice, for the case of bond percolation, Eqs. (92) to (96), are the same as the ones for the site percolation, Eqs. (33), (34) and (36) to (38), except for the factors  $p$  for the bare cases of the two and three-point functions. This simple fact implies the change of the non-universal constant  $\hat{A}$ . All the diverging integrals, together with their numerical prefactors are kept unaltered, thus the critical exponents are the same. All the details of the computation of the non-universal constants can be found in App. (A).

## 7 Conclusions

In this article we have shown how to obtain recover, at one-loop level of approximation, the results of the  $\epsilon$ -expansion for the critical exponents of the percolation problem on a  $D$ -dimensional regular lattice, by means of a new method, the  $M$ -layer construction. To do so, we computed the observables of interest for the case of site percolation in the non-percolating phase — the two- and three-point correlation functions, i.e. the probability that two or three sites belong to the same cluster — in properly chosen graphs at the leading orders. We then computed the  $\epsilon$ -expansion for the critical exponents, recovering, at first order, the same values already obtained for bond percolation using the  $n \rightarrow 0$  continuation of the field theory applied to the Potts model with  $n + 1$  states. Moreover, we have shown that within the  $M$ -layer construction the bond percolation problem differs from site percolation only for non-universal constants, which directly implies the universality between site and bond percolation in any dimension  $D$ . The analysis presented here clearly illustrate that the  $M$ -layer construction effectively allows one to extract quantitative information on the critical behavior even for problems, such as percolation, which are not defined by a Hamiltonian.

We explained for the first time how this method can be applied to a known problem in order to obtain the  $\epsilon$ -expansion of the critical exponents. Recent studies have utilized the  $M$ -layer construction to derive non-trivial insights into models whose critical behavior is not yet completely understood [14–18, 26], or to show that for well-known problems the one-loop results align with those from standard field theory [13, 24]. In this paper, we advance this approach a step forward by showing how, applying the standard theoretical recipes of the renormalization group, one can extract the critical series of the critical exponents. We believe this investigation could be highly beneficial in guiding the computation of critical exponents for problems where the standard RG approach is inapplicable [18].

Regarding the specific problem of percolation, it would be interesting to extend the calculations made in this work for the percolating phase  $p > p_c$ . In this sense, the preliminary calculation of the Ginzburg criterion at the bare order (i.e. without loops) has already been done using the  $M$ -layer construction, obtaining the known upper critical dimension,  $D_U = 6$  [27]. To proceed further and obtain the values of the critical exponents in the non-percolating phase, it is necessary to calculate the same observables as Ref. [27] with the corrections due to the one-loop structures. We leave this analysis to future work.

## A Identification of the constants in the $M$ -layer expansion

In this section we generalize the computation of the main text for the two and three-point function, with the goal of identifying the least number of constants that describe the loop expansion due to the  $M$ -layer construction. To start with we write all the contributions, in Fourier space, of a generic  $V_e$ -point correlation, computed on a generic topology,  $\mathcal{G}$ , with  $I$  lines,  $V_e$  external points,  $V_i$  internal vertices,  $N_{loop}$  number of loops:

$$\begin{aligned} \overline{\widehat{C}_{V_e}(\{k_j\})} \Big|_{\mathcal{G}} &= \frac{1}{S(\mathcal{G}) M^{N_{loop}+V_e-1}} (2D)^{V_e} \left( \frac{(2D)!}{(2D-3)!} \right)^{V_i} \left( \prod_{i=1}^I \int dL_i \right) \times \\ &\times (2\pi)^D \delta^D \left( \sum_{j=1}^{V_e} k_j \right) a_l^{-DV_i} \left( \int \prod_{l=1}^{N_{loop}} \frac{d^D q_l}{(2\pi)^D} \right) \left( \prod_{i=1}^I \widehat{\mathcal{N}}_{L_i}(\{q_l\}, \{k_j\}) \right) p^{I-2V_i} f(\mathcal{C}_{V_e,lc}) p^{\sum_{i=1}^I L_i}, \end{aligned} \quad (97)$$

with the same convention for the Fourier transform used in the main text, Eq. (40). Notice that  $\widehat{\mathcal{N}}_L$  are functions of linear combinations  $g_i(\{q_l\}, \{k_j\})$  of internal  $(\{q_l\}$  for  $l = 1, \dots, N_{loop})$  and external momenta  $(\{k_j\}$  for  $j = 1, \dots, V_e)$ , that ensure momentum conservation at each vertex. The factor  $p^{I-2V_i}$  and the function  $f(\mathcal{C}_{V_e,lc})$  come from Eqs. (33), (34), (36), (37) and (38). The first is the eventual extra factor  $p$ , which is present only for  $\mathcal{C}_{2,lc}(\mathcal{G}_1; L)$  and  $\mathcal{C}_{3,lc}(\mathcal{G}_3; )$ , as can be checked by substituting the corresponding values for  $I$  and  $V_i$  (notice that the specific expression,  $p^{I-2V_i}$ , is valid only for three-degree vertices, for  $V_i$   $d$ -degree vertices it is  $p^{I-(d-1)V_i}$  and can be generalized if vertices of different degree are present). The same goes for the factor  $(2D-3)!$ , whose generalization for a  $d$ -degree vertex is  $(2D-d)!$ . The function  $f(\mathcal{C}_{V_e,lc})$  assumes the following values:

$$f(\mathcal{C}_{2,lc}(\mathcal{G}_1; L)) = 1, \quad (98)$$

$$f(\mathcal{C}_{2,lc}(\mathcal{G}_2; \vec{L})) = -1, \quad (99)$$

$$f(\mathcal{C}_{3,lc}(\mathcal{G}_3; \vec{L}')) = 1, \quad (100)$$

$$f(\mathcal{C}_{3,lc}(\mathcal{G}_4; \vec{L}'')) = -2, \quad (101)$$

$$f(\mathcal{C}_{3,lc}(\mathcal{G}_5; \vec{L}''')) = -1. \quad (102)$$

Notice that the diagrams we computed in this work are of the form of Eq. (97). We believe that higher order diagrams (with three-degree vertices only) for a generic  $V_e$ -point function obey it as well, but this hypothesis is not necessary for the results described in this paper.

Next, using the asymptotic expression of the NBP in Fourier space, Eq. (43), together with the rescaling of momenta and lengths, in Eq. (50), we arrive at

$$\begin{aligned} \overline{\widehat{C}_{V_e}(\{k_j\})} \Big|_{\mathcal{G}} &= \frac{1}{S(\mathcal{G}) M^{N_{loop}-1+V_e}} (2D)^{V_e} \left( \frac{(2D)!}{(2D-3)!} \right)^{V_i} \mu^{-I} \left( \prod_{i=1}^I \int d\widehat{L}_i \right) \times \\ &\times (2\pi)^D \delta^D \left( \sum_{j=1}^{V_e} k_j \right) a_l^{-DV_i} \left( \int \prod_{l=1}^{N_{loop}} \frac{d^D \widehat{q}_l}{(2\pi)^D} \right) p^{I-2V_i} f(\mathcal{C}_{V_e,lc}) \times \\ &\times \left( \frac{\mu(2D-2)}{a_l^2} \right)^{\frac{D}{2}(N_{loop}-1)} \left( \frac{\mu(2D-2)}{a_l^2} \right)^{\frac{D}{2}} \left( \frac{2D}{2D-1} \right)^I \prod_{i=1}^I e^{-g_i(\{\widehat{q}_l\}, \{\widehat{k}_j\})^2 \widehat{L}_i - \widehat{L}_i} a_l^{ID}, \end{aligned} \quad (103)$$

where  $\widehat{k}$  is a function of  $k$  according to (50). Note that, as done in the main text, we did not rescale the external momenta inside the delta function.

Given the known relations for  $V_i$ ,  $V_e$ ,  $I$  and  $N_{loop}$  in a generic diagram with internal vertices of degree three:

$$V_i = V_e + 2(N_{loop} - 1) \quad \text{and} \quad I = 2V_e + 3(N_{loop} - 1), \quad (104)$$

in Eq. (103) we can identify the following topology-dependent term:

$$\frac{1}{S(\mathcal{G})} \left( \prod_{i=1}^I \int d\widehat{L}_i \right) \left( \int \prod_{l=1}^{N_{loop}} \frac{d^D \widehat{q}_l}{(2\pi)^D} \right) f(\mathcal{C}_{V_e, lc}) \prod_{i=1}^I e^{-g_i(\{\widehat{q}_l\}, \{\widehat{k}_j\})^2 \widehat{L}_i - \widehat{L}_i}. \quad (105)$$

and the following three factors:

- a constant to the power  $(N_{loop} - 1)$ :

$$\frac{1}{M} \left( \frac{(2D)!}{(2D-3)!} \right)^2 p^{-1} (2D-2)^{\frac{D}{2}} \left( \frac{2D}{2D-1} \right)^3 \mu^{\frac{D}{2}-3} \equiv \widehat{A} \mu^{\frac{D}{2}-3}, \quad (106)$$

- a constant to the power  $V_e$ :

$$\frac{1}{M} 2D \left( \frac{(2D)!}{(2D-3)!} \right) \left( \frac{2D}{2D-1} \right)^2 a_l^D \mu^{-2} \equiv \widehat{B} a_l^D \mu^{-2}, \quad (107)$$

- an overall factor:

$$(2\pi)^D \delta^D \left( \sum_{j=1}^{V_e} k_j \right) \left( \frac{\mu(2D-2)}{a_l^2} \right)^{\frac{D}{2}} \equiv (2\pi)^D \delta^D \left( \sum_{j=1}^{V_e} k_j \right) \mu^{D/2} \widehat{C} a_l^{-D}, \quad (108)$$

as defined in Eqs. (47), (48) and (49). With the expression given in Eq. (103) it is possible to easily identify the relevant constants to perform the expansion in inverse powers of  $M$ . Notice that these are all non-universal constants, as directly shown for the case of the bond percolation problem in the main text.

## B Connection with field theoretical expressions

In this section we show how to write the expressions for  $\widehat{C}_{2,lc}(k, k')$  and  $\widehat{C}_{3,lc}(k_1, k_2, k_3)$ , Eqs. (45) and (46), in terms of scalar propagators, as in the corresponding field theory. To do so, starting from the mentioned equations, we first perform the integrals over the lengths with lower and upper limits of integration respectively  $\mu/\Lambda^2$  and  $\infty$ . Notice that we are interested in the critical behavior, that is for  $\mu \rightarrow 0$ , thus we can set the lower limit to 0, that amount to neglect higher orders in  $\mu$ . The results are

$$\begin{aligned} \widehat{C}_2(k, k') &= \frac{\widehat{C} \widehat{B}^2 a_l^D}{\widehat{A} \mu} \frac{1}{\widehat{k}^2 + 1} (2\pi)^D \delta^D(k + k') \times \\ &\times \left( 1 - \frac{\widehat{A} \mu^{\frac{D}{2}-3}}{2(\widehat{k}^2 + 1)} \int \frac{d^D \widehat{q}}{(2\pi)^D} \frac{1}{1 + (\widehat{k} - \widehat{q})^2} \frac{1}{1 + \widehat{q}^2} \right) + \mathcal{O}\left(\frac{1}{M^3}\right) \end{aligned} \quad (109)$$

$$\begin{aligned} \overline{\widehat{C}_3(k_1, k_2, k_3)} &= \frac{\widehat{C}\widehat{B}^3 a_l^{2D}}{\widehat{A}\mu^3} \frac{(2\pi)^D \delta^D(k_1 + k_2 + k_3)}{(\widehat{k}_1^2 + 1)(\widehat{k}_2^2 + 1)(\widehat{k}_3^2 + 1)} \times \\ &\left( 1 - 2\widehat{A}\mu^{\frac{D}{2}-3} \int \frac{d^D \widehat{q}}{(2\pi)^D} \frac{1}{1 + (\widehat{k}_2 + \widehat{k}_3 + \widehat{q})^2} \frac{1}{1 + (\widehat{k}_2 + \widehat{q})^2} \frac{1}{1 + \widehat{q}^2} + \right. \\ &\left. - \frac{1}{2} \frac{\widehat{A}\mu^{\frac{D}{2}-3}}{(\widehat{k}_2 + \widehat{k}_3)^2 + 1} \int \frac{d^D \widehat{q}}{(2\pi)^D} \frac{1}{1 + (\widehat{k}_2 + \widehat{q})^2} \frac{1}{1 + \widehat{q}^2} + perm. \right) + \mathcal{O}\left(\frac{1}{M^4}\right). \end{aligned} \quad (110)$$

Next we rescale the momenta and we define the bare mass and coupling, respectively  $m_b$  and  $g_b$ , according to:

$$\widetilde{k} \equiv \mu^{\frac{1}{2}} a_l^{\frac{2D}{D+2}} \widehat{A}^{\frac{1}{D+2}} \widehat{B}^{-\frac{2}{D+2}} \widehat{k} \quad (111)$$

$$m_b^2 \equiv \mu a_l^{-\frac{4D}{D+2}} \widehat{A}^{\frac{2}{D+2}} \widehat{B}^{-\frac{4}{D+2}} \quad (112)$$

$$g_b \equiv a_l^{D\frac{D-6}{D+2}} \widehat{A}^{\frac{4}{D+2}} \widehat{B}^{\frac{D-6}{D+2}} \widehat{C}^{-2+\frac{3}{D}+\frac{D}{4}} \quad (113)$$

and we obtain

$$\begin{aligned} \overline{\widehat{C}_2(\widetilde{k}, \widetilde{k}')} &= (2\pi)^D \delta^D(k + k') \times \\ &\times \left( \frac{1}{\widetilde{k}^2 + m_b^2} - \frac{1}{2} g_b^2 \frac{1}{(\widetilde{k}^2 + m_b^2)^2} \int \frac{d^D \widetilde{q}}{(2\pi)^D} \frac{1}{(\widetilde{k} - \widetilde{q})^2 + m_b^2} \frac{1}{\widetilde{q}^2 + m_b^2} \right) + \mathcal{O}\left(\frac{1}{M^3}\right) \end{aligned} \quad (114)$$

$$\begin{aligned} \overline{\widehat{C}_3(k_1, k_2, k_3)} &= \frac{1}{(\widetilde{k}_1^2 + m_b^2)(\widetilde{k}_2^2 + m_b^2)(\widetilde{k}_3^2 + m_b^2)} (2\pi)^D \delta^D(\widetilde{k}_1 + \widetilde{k}_2 + \widetilde{k}_3) \times \\ &\times \left( g_b - 2g_b^3 \int \frac{d^D \widetilde{q}}{(2\pi)^D} \frac{1}{(\widetilde{k}_2 + \widetilde{k}_3 + \widetilde{q})^2 + m_b^2} \frac{1}{(\widetilde{k}_2 + \widetilde{q})^2 + m_b^2} \frac{1}{\widetilde{q}^2 + m_b^2} + \right. \\ &\left. - \frac{1}{2} g_b^3 \frac{1}{(\widetilde{k}_2 + \widetilde{k}_3)^2 + m_b^2} \int \frac{d^D \widetilde{q}}{(2\pi)^D} \frac{1}{(\widetilde{k}_2 + \widetilde{q})^2 + m_b^2} \frac{1}{\widetilde{q}^2 + m_b^2} + perm. \right) + \mathcal{O}\left(\frac{1}{M^4}\right), \end{aligned} \quad (115)$$

which are the results of the corresponding field theory associated to the percolation problem [7, 9].

As a last remark we notice that it is not always possible to write the results of the  $M$ -layer construction in terms of scalar propagators. For the percolation, problem the observables computed on a given topology, such as Eqs. (33) or (34), are powers of the probability  $p$  to some combination of the lengths of the lines, thus the integrals over the lengths give the scalar propagator factor. For a generic problem the expressions of the observables can be more complicated functions of the lengths (see Refs. [17, 28] as an example) and the corresponding integrals do not give the simple structure of a scalar propagator. On the other hand, for simple problems, whose field theoretical analysis is clear, the propagator structure is recovered by means of the  $M$ -layer construction [24].

It is also interesting to note that the integrals occurring in field theories are *actually computed* through the application of formulas like the following:

$$\frac{1}{k^2 + m^2} = \int_0^\infty e^{-l(k^2 + m^2)} dl \quad (116)$$

see *e.g.* the appendix to chapter five in [20] and this amount to back from Eqs. (109) and (110) back to Eqs. (45) and (46). Thus the  $M$ -layer approach gives directly expressions in the above treatable form. Furthermore the integration variable  $l$ , that seems artificial in field theory, has instead the natural meaning of the length of the internal lines of the diagrams in the  $M$ -layer approach.

## C Other diagrams

In this appendix we take into account another possible diagrams of order  $\mathcal{O}(1/M^2)$  that may contribute to the two-point correlation. As discussed in [24], the computation of the line without loop should be corrected to  $\mathcal{O}(1/M^2)$  by diagram  $\mathcal{G}'_1$  in Fig. 3, with the corresponding weight:  $W(\mathcal{G}'_1) = 1/M(1 - 1/M)$ .

While the contribution of  $\mathcal{G}'_1$  at order  $\mathcal{O}(1/M)$  is already included in Eq. (35), its contribution at order  $\mathcal{O}(1/M^2)$  is not included in Eq. (35) because  $\mathcal{G}'_1$  diverges with a lower power of  $\mu$  with respect to  $\mathcal{G}_2$ , which also contributes at order  $\mathcal{O}(1/M^2)$ .

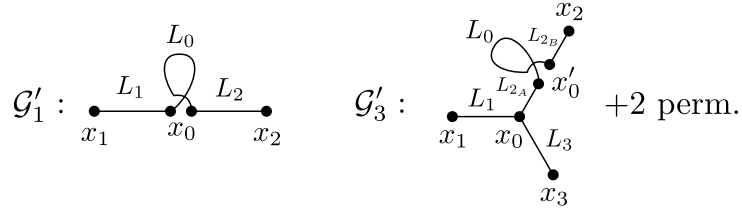


Figure 3: Less divergent diagrams that contribute to the two-point function. Notice that the two couple of vertices in  $x_0$  and  $x'_0$  belong to two different layers while on the projection they are superimposed. The two lines with length  $L_0$  coils themselves in the  $M$ -layer lattice, in such a way that the projection on the original lattice looks like a loop.

The contribution of  $\mathcal{G}'_1$  at order  $\mathcal{O}(1/M^2)$  is

$$-\frac{(2D)^2}{M^2} \frac{(2D)!}{(2D-4)!} \sum_{L_1, L_0, L_2} \sum_{x_0} \mathcal{N}_{L_1}(x_1, x_0) \mathcal{N}_{L_0}(x_0, x_0) \mathcal{N}_{L_2}(x_0, x_2) \mathcal{C}_{2,lc}(\mathcal{G}'_1; L_1, L_0, L_2), \quad (117)$$

where

$$\mathcal{C}_{2,lc}(\mathcal{G}'_1; L_1, L_0, L_2) = \mathcal{C}_{2,lc}(\mathcal{G}_1; L_1 + L_0 + L_2) = p p^{L_1 + L_0 + L_2}. \quad (118)$$

In Fourier space, using Eqs. (42) and (43), it becomes:

$$-(2\pi)^D \delta^D(k_1 + k_2) \frac{(2D)^2}{M^2} \frac{(2D)!}{(2D-4)!} \left( \frac{2D}{2D-1} \right)^3 a_l^{2D} p \frac{1}{\frac{a_l^2}{2D-2} k_1^2 + \mu} \frac{1}{\frac{a_l^2}{2D-2} k_2^2 + \mu} \times \\ \times \int \frac{d^D k_0}{(2\pi)^D} \int_{\mu/\Lambda^2}^{\infty} d\hat{L}_0 e^{-\left( \frac{a_l^2}{\mu(2D-2)} k_0^2 + 1 \right) \hat{L}_0},$$

which can be rewritten scaling all the momenta,  $\hat{k} \equiv k \frac{a_l}{\sqrt{\mu(2D-2)}}$ , apart from the ones in the delta function, as:

$$\begin{aligned}
 & -(2\pi)^D \delta^D(k_1 + k_2) \frac{(2D)^2}{M^2} \frac{(2D)!}{(2D-4)!} \left( \frac{2D}{2D-1} \right)^3 \mu^{\frac{D}{2}-3} \frac{a_l^D p(2D-2)^{\frac{D}{2}}}{(\widehat{k}_1^2 + 1)(\widehat{k}_2^2 + 1)} \times \\
 & \times \int \frac{d^D \widehat{k}_0}{(2\pi)^D} \frac{1}{\widehat{k}_0^2 + 1} \propto \frac{\mu^{\frac{D}{2}-3}}{M^2},
 \end{aligned}$$

where, as usual, we neglected higher orders in  $\mu$  setting the lower limit of the length integration to 0. The other contribution to order  $\mathcal{O}(1/M^2)$  is from diagram  $\mathcal{G}_2$ , repeating the same steps we have

$$\begin{aligned}
 & -(2\pi)^D \delta^D(k_1 + k_2) \frac{(2D)^2}{2M^2} \left( \frac{(2D)!}{(2D-3)!} \right)^2 \left( \frac{2D}{2D-1} \right)^4 \mu^{\frac{D}{2}-4} \frac{a_l^D (2D-2)^{\frac{D}{2}}}{(\widehat{k}_1^2 + 1)(\widehat{k}_2^2 + 1)} \times \\
 & \times \int \frac{d^D \widehat{k}}{(2\pi)^D} \frac{1}{\widehat{k}^2 + 1} \frac{1}{(\widehat{k}_1 - \widehat{k})^2 + 1} \propto \frac{\mu^{\frac{D}{2}-4}}{M^2},
 \end{aligned}$$

from which it is clear that near the critical point,  $\mu \sim 0$ , the contribution of  $\mathcal{G}'_1$  can be neglected with respect to the one of  $\mathcal{G}_2$ . Analogously, diagram  $\mathcal{G}'_3$ , is negligible with respect to  $\mathcal{G}_4$  and  $\mathcal{G}_5$ . Thus the computations for the three-point correlation function of the main text gives the correct critical behavior.

It is also possible to generalize this argument, at least for the case of the percolation problem. Since for each line of the diagram a factor proportional to  $\mu^{-1}(\widehat{k}^2 + 1)^{-1}$  appears, we understand that, at a given order in  $\mathcal{O}(1/M)$  the most divergent diagrams, in the limit  $\mu \rightarrow 0$  are the ones with the largest number of lines.

This argument is not valid generally for any problem or model. Indeed, the computation of the observables on a given diagram is the only model-dependent part of the  $M$ -layer procedure and in general the result can be a non-trivial function of the lengths, as we noticed in the end of appendix B.

## D Four-point correlation function

We present, in this appendix, the computation for the most divergent contributions to the four-point correlation function. All the possible topologies, with only three and four-degree vertices, are shown in Fig. 4.

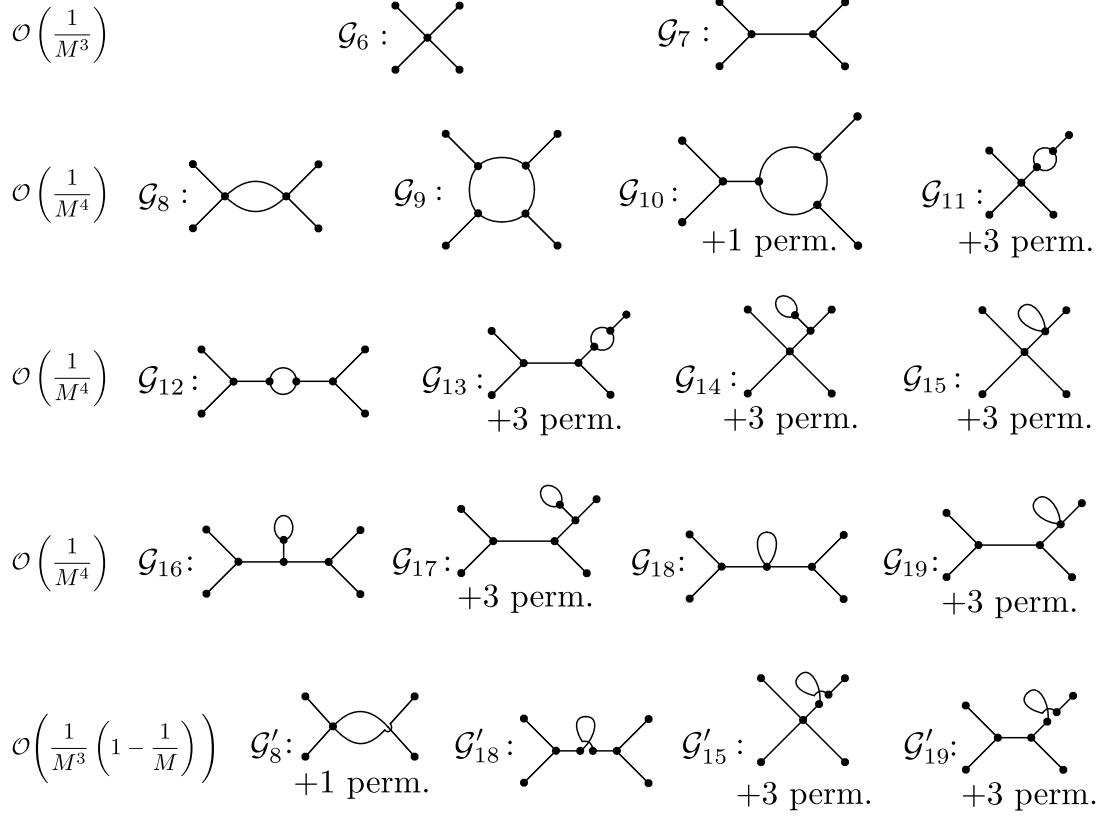


Figure 4: Diagrams that contribute to the four-point correlation functions up to one loop.

Along the lines of the reasoning given for neglecting  $\mathcal{G}'_1$  with respect to  $\mathcal{G}_2$  we identify the most divergent diagrams to each  $\mathcal{O}(1/M)$  order for the four-point correlation function simply considering the diagrams with the largest number of lines. It turns out that the relevant diagrams, for the four-point function, are the ones shown in Fig. 5:  $\mathcal{G}_7$  to order  $\mathcal{O}(1/M^3)$ ,  $\mathcal{G}_9$ ,  $\mathcal{G}_{12}$  and  $\mathcal{G}_{13}$  to order  $\mathcal{O}(1/M^4)$ . Notice that, in principle, we should have considered also diagrams with vertices of degree larger than four, but they all have, at one loop order, less lines than the ones we included in Fig. 5, thus they are less divergent near the critical point  $\mu \sim 0$ .



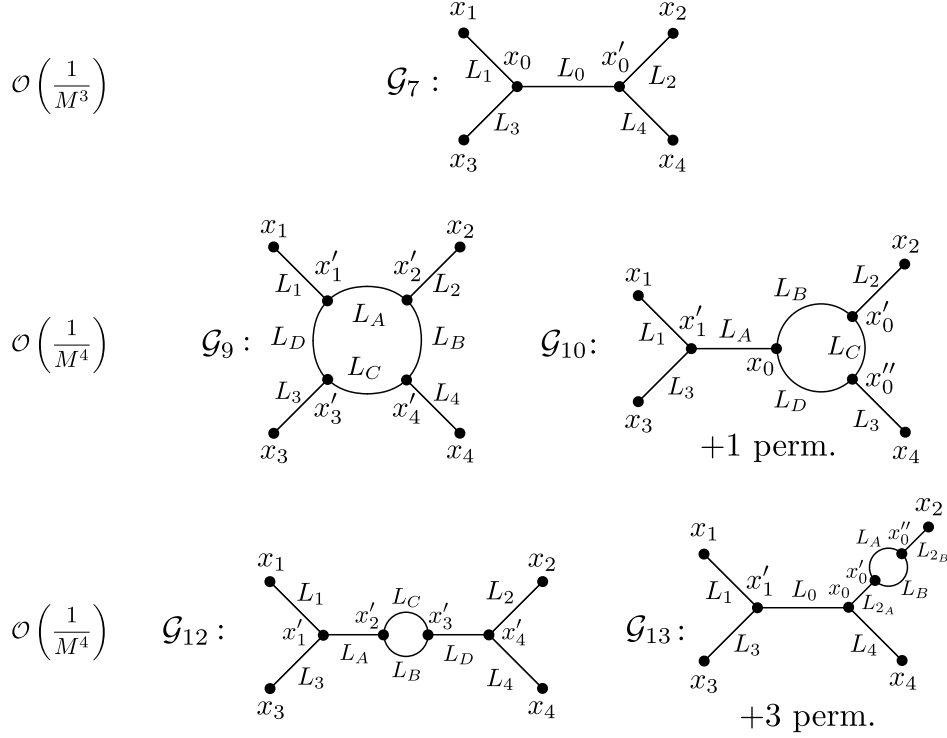


Figure 5: Most divergent diagrams contributing to the four-point correlation functions up to one loop near the critical point.

Now we can write the contributions of the identified diagrams:

$$\begin{aligned}
 \overline{C_4(x_1, x_2, x_3, x_4)} = & \quad (119) \\
 & \frac{1}{M^3} \sum_{\vec{L}} \sum_{x_0, x'_0} \mathcal{N}(\mathcal{G}_7; \vec{L}; x_1, x_2, x_3, x_4, x_0, x'_0) \mathcal{C}_{4,lc}(\mathcal{G}_7; \vec{L}) + \\
 & + \frac{1}{M^4} \sum_{\vec{L}'} \sum_{\{x'_i\}, i=1, \dots, 4} \mathcal{N}(\mathcal{G}_9; \vec{L}'; x_1, x_2, x_3, x_4, x'_1, x'_2, x'_3, x'_4) \mathcal{C}_{4,lc}(\mathcal{G}_9; \vec{L}') + \\
 & + \frac{1}{M^4} \sum_{\vec{L}'} \sum_{x'_1, x_0, x'_0, x''_0} \mathcal{N}(\mathcal{G}_{10}; \vec{L}'; x_1, x_2, x_3, x_4, x'_1, x_0, x'_0, x''_0) \mathcal{C}_{4,lc}(\mathcal{G}_{10}; \vec{L}') + \\
 & + \frac{1}{2M^4} \sum_{\vec{L}'} \sum_{\{x'_i\}, i=1, \dots, 4} \mathcal{N}(\mathcal{G}_{12}; \vec{L}'; x_1, x_2, x_3, x_4, x'_1, x'_2, x'_3, x'_4) \mathcal{C}_{4,lc}(\mathcal{G}_{12}; \vec{L}') + \\
 & + \frac{1}{2M^4} \sum_{\vec{L}''} \sum_{x'_1, x_0, x'_0, x''_0} \mathcal{N}(\mathcal{G}_{13}; \vec{L}''; x_1, x_2, x_3, x_4, x'_1, x_0, x'_0, x''_0) \mathcal{C}_{4,lc}(\mathcal{G}_{13}; \vec{L}'') + \\
 & + \mathcal{O}\left(\frac{1}{M^5}\right),
 \end{aligned}$$

where  $\vec{L} = (L_0, L_1, L_2, L_3, L_4)$ ,  $\vec{L}' = (L_1, L_2, L_3, L_4, L_A, L_B, L_C, L_D)$ ,  $\vec{L}'' = (L_1, L_3, L_4, L_{2A}, L_{2B}, L_A, L_B, L_C, L_D)$ ,

$$\begin{aligned}
 \mathcal{N}(\mathcal{G}_7; \vec{L}; x_1, x_2, x_3, x_4, x_0, x'_0) &= (2D)^4 \left( \frac{(2D)!}{(2D-3)!} \right)^2 \prod_{i=1,3} \mathcal{N}_{L_i}(x_i, x_0) \prod_{i=2,4} \mathcal{N}_{L_i}(x_i, x_0) \mathcal{N}_{L_0}(x_0, x'_0), \\
 \mathcal{N}(\mathcal{G}_9; \vec{L}'; x_1, x_2, x_3, x_4, x'_1, x'_2, x'_3, x'_4) &= (2D)^4 \left( \frac{(2D)!}{(2D-3)!} \right)^4 \times \\
 &\times \prod_{i=1}^4 \mathcal{N}_{L_i}(x_i, x'_i) \mathcal{N}_{L_A}(x'_1, x'_2) \mathcal{N}_{L_B}(x'_2, x'_4) \mathcal{N}_{L_C}(x'_3, x'_4) \mathcal{N}_{L_D}(x'_3, x'_1),
 \end{aligned}$$

$$\mathcal{N}(\mathcal{G}_{10}; \vec{L}'; x_1, x_2, x_3, x_4, x'_1, x_0, x'_0, x''_0) = (2D)^4 \left( \frac{(2D)!}{(2D-3)!} \right)^4 \times \\ \times \prod_{i=1}^4 \mathcal{N}_{L_i}(x_i, x'_i) \mathcal{N}_{L_A}(x'_1, x_0) \mathcal{N}_{L_B}(x_0, x'_0) \mathcal{N}_{L_C}(x'_0, x''_0) \mathcal{N}_{L_D}(x_0, x''_0),$$

$$\mathcal{N}(\mathcal{G}_{12}; \vec{L}'; x_1, x_2, x_3, x_4, x'_1, x'_2, x'_3, x'_4) = (2D)^4 \left( \frac{(2D)!}{(2D-3)!} \right)^4 \times \\ \times \mathcal{N}_{L_1}(x_1, x'_1) \mathcal{N}_{L_2}(x_2, x'_2) \mathcal{N}_{L_3}(x_3, x'_3) \mathcal{N}_{L_4}(x_4, x'_4) \mathcal{N}_{L_A}(x'_1, x'_2) \mathcal{N}_{L_B}(x'_2, x'_3) \mathcal{N}_{L_C}(x'_3, x'_4) \mathcal{N}_{L_D}(x'_4, x'_3)$$

$$\mathcal{N}(\mathcal{G}_{13}; \vec{L}''; x_1, x_2, x_3, x_4, x'_1, x_0, x'_0, x''_0) = (2D)^4 \left( \frac{(2D)!}{(2D-3)!} \right)^4 \times \\ \times \mathcal{N}_{L_1}(x_1, x'_1) \mathcal{N}_{L_3}(x_3, x'_1) \mathcal{N}_{L_4}(x_4, x_0) \mathcal{N}_{L_0}(x'_1, x_0) \mathcal{N}_{L_{2B}}(x_2, x''_0) \mathcal{N}_{L_{2A}}(x_0, x'_0) \mathcal{N}_{L_A}(x'_0, x''_0) \mathcal{N}_{L_B}(x'_0, x''_0) \\ \text{and}$$

$$\mathcal{C}_{4,lc}(\mathcal{G}_7; \vec{L}) = p p^{L_1+L_2+L_3+L_4+L_0}; \quad (120)$$

$$\mathcal{C}_{4,lc}(\mathcal{G}_9; \vec{L}') = -3 p^{L_1+L_2+L_3+L_4+L_A+L_B+L_C+L_D}; \quad (121)$$

$$\mathcal{C}_{4,lc}(\mathcal{G}_{10}; \vec{L}') = -2 p^{L_1+L_2+L_3+L_4+L_A+L_B+L_C+L_D}; \quad (122)$$

$$\mathcal{C}_{4,lc}(\mathcal{G}_{12}; \vec{L}') = -p^{L_1+L_2+L_3+L_4+L_A+L_B+L_C+L_D}; \quad (123)$$

$$\mathcal{C}_{4,lc}(\mathcal{G}_{13}; \vec{L}'') = -p^{L_1+L_3+L_4+L_0+L_{2A}+L_{2B}+L_A+L_B}. \quad (124)$$

Since the diagrams identified,  $\mathcal{G}_7$ ,  $\mathcal{G}_9$ ,  $\mathcal{G}_{10}$ ,  $\mathcal{G}_{12}$  and  $\mathcal{G}_{13}$ , contain only three-degree vertices, this allows us to use the generic equation derived in App. A for this kind of vertices, Eq. (103), where

$$f(\mathcal{C}_{4,lc}(\mathcal{G}_7; \vec{L}', L_4, L_0)) = 1, \quad (125)$$

$$f(\mathcal{C}_{4,lc}(\mathcal{G}_9; \vec{L})) = -3, \quad (126)$$

$$f(\mathcal{C}_{4,lc}(\mathcal{G}_{10}; \vec{L})) = -2, \quad (127)$$

$$f(\mathcal{C}_{4,lc}(\mathcal{G}_{12}; \vec{L}'')) = -1 = f(\mathcal{C}_{4,lc}(\mathcal{G}_{13}; \vec{L}''')) \quad (128)$$

and  $S(\mathcal{G}_7) = S(\mathcal{G}_9) = S(\mathcal{G}_{10}) = 1$ ,  $S(\mathcal{G}_{12}) = 2 = S(\mathcal{G}_{13})$ :

$$\overline{\widehat{C}_{4,lc}(\{k_i\}_{i=1,\dots,4})} = (2\pi)^D \delta^D \left( \sum_{i=1}^4 k_i \right) \frac{\widehat{B}^4 a_l^{3D} \widehat{C}}{\widehat{A} \mu^5} \prod_{i=1}^4 \frac{1}{\widehat{k}_i^2 + 1} \left( \int d\widehat{L}_0 e^{-\widehat{L}_0 - (\widehat{k}_1 + \widehat{k}_3)^2 \widehat{L}_0} + \right. \\ - 3 \widehat{A} \mu^{\frac{D}{2}-3} \prod_{i=A,B,C,D} \int d\widehat{L}_i e^{-\widehat{L}_i} \int \frac{d^D \widehat{q}}{(2\pi)^D} e^{-\widehat{q}^2 \widehat{L}_A - (\widehat{q} + \widehat{k}_2)^2 \widehat{L}_B - (\widehat{q} + \widehat{k}_2 + \widehat{k}_3)^2 \widehat{L}_C - (\widehat{k}_1 - \widehat{q})^2 \widehat{L}_D} \\ - 2 \widehat{A} \mu^{\frac{D}{2}-3} \prod_{i=A,B,C,D} \int d\widehat{L}_i e^{-\widehat{L}_i} e^{-(\widehat{k}_1 + \widehat{k}_3)^2 \widehat{L}_A} \int \frac{d^D \widehat{q}}{(2\pi)^D} e^{-\widehat{q}^2 \widehat{L}_B - (\widehat{q} + \widehat{k}_2)^2 \widehat{L}_C - (\widehat{q} + \widehat{k}_2 + \widehat{k}_4)^2 \widehat{L}_D} \\ - 2 \widehat{A} \mu^{\frac{D}{2}-3} \prod_{i=A,B,C,D} \int d\widehat{L}_i e^{-\widehat{L}_i} e^{-(\widehat{k}_2 + \widehat{k}_4)^2 \widehat{L}_A} \int \frac{d^D \widehat{q}}{(2\pi)^D} e^{-\widehat{q}^2 \widehat{L}_B - (\widehat{q} - \widehat{k}_1)^2 \widehat{L}_C - (\widehat{q} - \widehat{k}_1 - \widehat{k}_3)^2 \widehat{L}_D} \\ - \frac{\widehat{A} \mu^{\frac{D}{2}-3}}{2} \prod_{i=A,B,C,D} \int d\widehat{L}_i e^{-\widehat{L}_i} e^{-(\widehat{k}_1 + \widehat{k}_3)^2 (\widehat{L}_A + \widehat{L}_D)} \int \frac{d^D \widehat{q}}{(2\pi)^D} e^{-\widehat{q}^2 \widehat{L}_B - (\widehat{q} - \widehat{k}_1 - \widehat{k}_3)^2 \widehat{L}_C} \\ - \frac{\widehat{A} \mu^{\frac{D}{2}-3}}{2} \sum_{j=1}^4 \prod_{i=0,A,B,j_A,j_B} \int d\widehat{L}_i e^{-\widehat{L}_i} e^{-(\widehat{k}_1 + \widehat{k}_3)^2 \widehat{L}_0 - \widehat{k}_2^2 (\widehat{L}_{j_A} + \widehat{L}_{j_B})} \int \frac{d^D \widehat{q}}{(2\pi)^D} e^{-\widehat{q}^2 \widehat{L}_A - (\widehat{q} + \widehat{k}_j)^2 \widehat{L}_B} \Big) \\ + \mathcal{O} \left( \frac{1}{M^5} \right). \quad (129)$$

As for the two and three-point correlation functions, we define  $\chi_4(\mu)$  as the four-point correlation function at zero external momenta, divided by  $a_l^{3D}$  and without the factor  $(2\pi)^D \delta^D \left( \sum_{i=1}^4 k_i \right)$  :

$$\chi_4(\mu) = \frac{\widehat{B}^4 \widehat{C}}{\widehat{A} \mu^5} \left( 1 - \frac{5}{2} \frac{\widehat{A} \mu^{\frac{D}{2}-3}}{(4\pi)^{\frac{D}{2}}} I_\alpha(\mu) - 4 \frac{\widehat{A} \mu^{\frac{D}{2}-3}}{(4\pi)^{\frac{D}{2}}} I_\gamma(\mu) - 3 \frac{\widehat{A} \mu^{\frac{D}{2}-3}}{(4\pi)^{\frac{D}{2}}} I_\delta(\mu) \right) \quad (130)$$

where  $I_\alpha$  and  $I_\gamma$  are defined in Eqs. (60) and (66) respectively, while

$$I_\delta(\mu) \equiv \int_{\frac{\mu}{\lambda^2}}^{\infty} d\widehat{L}_A d\widehat{L}_B d\widehat{L}_C d\widehat{L}_D \frac{e^{-\widehat{L}_A - \widehat{L}_B - \widehat{L}_C - \widehat{L}_D}}{\left( \widehat{L}_A + \widehat{L}_B + \widehat{L}_C + \widehat{L}_D \right)^{\frac{D}{2}}}, \quad (131)$$

and consequently

$$\lim_{\mu \rightarrow 0} I_\delta(\mu) = \frac{6-D}{12} \Gamma \left( 3 - \frac{D}{2} \right). \quad (132)$$

Using the relation between  $\mu$  and  $m^2$ , Eq. (63), we can write  $\chi_4$  as a function of  $m^2$

$$\chi_4(\mu(m^2)) = \frac{\widehat{B}^4 \widehat{C}^{\frac{10}{D}+1}}{\widehat{A} a_l^{10}} m^{-10} \left( 1 + \frac{5}{2} \frac{u}{(4\pi)^{\frac{D}{2}}} I_\beta(\mu(m^2)) + \right. \\ \left. - 4 \frac{u}{(4\pi)^{\frac{D}{2}}} I_\gamma(\mu(m^2)) - 3 \frac{u}{(4\pi)^{\frac{D}{2}}} I_\delta(\mu(m^2)) \right) \quad (133)$$

where  $u$  is the bare coupling constant, defined in Eq. (69). Now we can look at the scaling, near the critical point  $m^2 \rightarrow 0$ , of the four-point function

$$D_4(\lambda) \equiv \left. \frac{\partial \ln \chi_4(\mu(m^2 \simeq 0))}{\partial \ln m^2} \right|_{g \text{ fixed}}, \quad \chi_4(\mu(m^2 \simeq 0)) \propto m^{2D_4(\lambda_c)}. \quad (134)$$

Using the expression of  $\chi(m^2)$  we have

$$D_4(\lambda_c) = \frac{1}{42} \left( D(3D - 55) + 12 \right). \quad (135)$$

We can now compare with the scaling of the four-point function

$$\chi_4(\mu(m^2 \simeq 0)) \sim m^{2D_4(\lambda_c)}, \quad D_k(\lambda_c) = \frac{k}{4} \eta - \frac{k}{2} + \frac{D}{2} \left( 1 - \frac{k}{2} \right), \quad (136)$$

with  $k = 4$ , which gives the expected result of Eq. (89)

$$\eta_D = \frac{D-6}{21}. \quad (137)$$

## References

- [1] D. Stauffer and A. Aharony, *Introduction To Percolation Theory*, CRC Press (1994).
- [2] K. Christensen and N. R. Moloney, *Complexity and criticality*, vol. 1, World Scientific Publishing Company (2005).

- [3] J. W. Essam, *Percolation theory*, Reports on Progress in Physics **43**(7), 833 (1980), doi:10.1088/0034-4885/43/7/001.
- [4] A. Aharony, *Universal critical amplitude ratios for percolation*, Phys. Rev. B **22**, 400 (1980), doi:10.1103/PhysRevB.22.400.
- [5] P. Kasteleyn and C. Fortuin, *Phase transitions in lattice systems with random local properties*, Physical Society of Japan Journal Supplement **26**, 11 (1969).
- [6] A. B. Harris, T. C. Lubensky, W. K. Holcomb and C. Dasgupta, *Renormalization-group approach to percolation problems*, Physical Review Letters **35**(6), 327 (1975).
- [7] D. J. Amit, *Renormalization of the potts model*, Journal of Physics A: Mathematical and General **9**(9), 1441 (1976), doi:10.1088/0305-4470/9/9/006.
- [8] R. Priest and T. Lubensky, *Critical properties of two tensor models with application to the percolation problem*, Physical Review B **13**(9), 4159 (1976).
- [9] O. F. de Alcantara Bonfim, J. E. Kirkham and A. J. McKane, *Critical exponents for the percolation problem and the yang-lee edge singularity*, Journal of Physics A: Mathematical and General **14**(9), 2391 (1981), doi:10.1088/0305-4470/14/9/034.
- [10] J. A. Gracey, *Four loop renormalization of  $\phi^3$  theory in six dimensions*, Phys. Rev. D **92**, 025012 (2015), doi:10.1103/PhysRevD.92.025012.
- [11] M. Borinsky, J. A. Gracey, M. V. Kompaniets and O. Schnetz, *Five-loop renormalization of  $\phi^3$  theory with applications to the lee-yang edge singularity and percolation theory*, Phys. Rev. D **103**, 116024 (2021), doi:10.1103/PhysRevD.103.116024.
- [12] A. Altieri, M. C. Angelini, C. Lucibello, G. Parisi, F. Ricci-Tersenghi and T. Rizzo, *Loop expansion around the bethe approximation through the  $m$ -layer construction*, Journal of Statistical Mechanics: Theory and Experiment **2017**(11), 113303 (2017), doi:10.1088/1742-5468/aa8c3c.
- [13] M. C. Angelini, G. Parisi and F. Ricci-Tersenghi, *One-loop topological expansion for spin glasses in the large connectivity limit*, Europhysics Letters **121**(2), 27001 (2018).
- [14] M. C. Angelini, C. Lucibello, G. Parisi, F. Ricci-Tersenghi and T. Rizzo, *Loop expansion around the bethe solution for the random magnetic field ising ferromagnets at zero temperature*, Proceedings of the National Academy of Sciences **117**, 2268 (2019).
- [15] T. Rizzo, *Fate of the hybrid transition of bootstrap percolation in physical dimension*, Phys. Rev. Lett. **122**, 108301 (2019), doi:10.1103/PhysRevLett.122.108301.
- [16] T. Rizzo and T. Voigtmann, *Solvable models of supercooled liquids in three dimensions*, Phys. Rev. Lett. **124**, 195501 (2020), doi:10.1103/PhysRevLett.124.195501.
- [17] M. C. Angelini, C. Lucibello, G. Parisi, G. Perrupato, F. Ricci-Tersenghi and T. Rizzo, *Unexpected upper critical dimension for spin glass models in a field predicted by the loop expansion around the bethe solution at zero temperature*, Phys. Rev. Lett. **128**, 075702 (2022), doi:10.1103/PhysRevLett.128.075702.
- [18] M. Baroni, G. G. Lorenzana, T. Rizzo and M. Tarzia, *Corrections to the bethe lattice solution of anderson localization*, Physical Review B **109**(17), 174216 (2024).
- [19] H. A. Bethe, *Statistical theory of superlattices*, Proceedings of the Royal Society of London. Series A-Mathematical and Physical Sciences **150**(871), 552 (1935).

- [20] G. Parisi, *Statistical field theory*, Addison-Wesley (1988).
- [21] J. Zinn-Justin, *Quantum Field Theory and Critical Phenomena*, Oxford University Press, ISBN 9780198509233, doi:10.1093/acprof:oso/9780198509233.001.0001 (2002).
- [22] A. Coniglio, *Geometrical approach to phase transitions in frustrated and unfrustrated systems*, Physica A: Statistical Mechanics and its Applications **281**(1-4), 129 (2000).
- [23] R. Fitzner and R. van der Hofstad, *Non-backtracking random walk*, Journal of Statistical Physics **150**, 264 (2013).
- [24] M. C. Angelini, S. Palazzi, G. Parisi and T. Rizzo, *Bethe  $m$ -layer construction on the ising model*, Journal of Statistical Mechanics: Theory and Experiment **2024**(6), 063301 (2024), doi:10.1088/1742-5468/ad526e.
- [25] J. Cardy, *Scaling and Renormalization in Statistical Physics*, Cambridge Lecture Notes in Physics. Cambridge University Press (1996).
- [26] M. Baroni, G. G. Lorenzana, T. Rizzo and M. Tarzia, *Corrections to the bethe lattice solution of anderson localization* (2023), 2304.10365.
- [27] G. Perrupato, M. C. Angelini, G. Parisi, F. Ricci-Tersenghi and T. Rizzo, *Ising spin glass on random graphs at zero temperature: Not all spins are glassy in the glassy phase*, Physical Review B **106**(17), 174202 (2022).
- [28] M. C. Angelini, C. Lucibello, G. Parisi, F. Ricci-Tersenghi and T. Rizzo, *Loop expansion around the bethe solution for the random magnetic field ising ferromagnets at zero temperature*, Proceedings of the National Academy of Sciences **117**(5), 2268 (2020), doi:10.1073/pnas.1909872117, <https://www.pnas.org/doi/pdf/10.1073/pnas.1909872117>.